

Sample Compression for Self-Certified Continual Learning

Jacob Comeau^{1,2}

Mathieu Bazinet^{1,2}

Pascal Germain^{1,2}

Cem Subakan^{1,2,3}

¹Département d'informatique et génie logiciel, Université Laval, Québec, Qc, Canada

²Mila - Quebec Artificial Intelligence Institute, Montreal, Qc, Canada

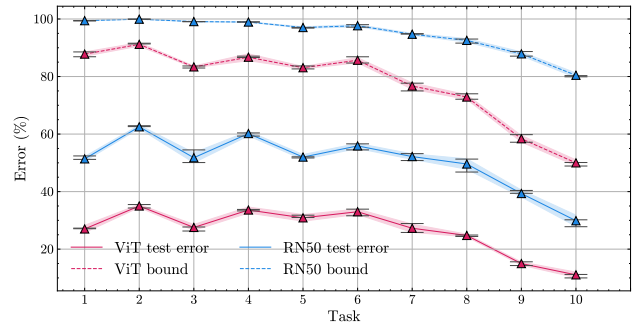
³Computer Science and Software Engineering Department, Concordia University, Montreal, Qc, Canada

Abstract

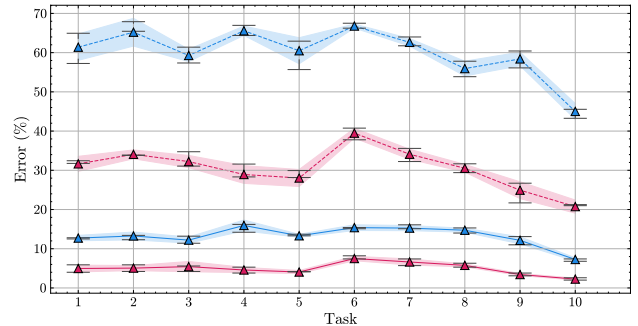
Continual learning algorithms aim to learn from a sequence of tasks. In order to avoid catastrophic forgetting, most existing approaches rely on heuristics and do not provide computable learning guarantees. In this paper, we introduce Continual Pick-to-Learn (CoP2L), a method grounded in sample compression theory that retains representative samples for each task in a principled and efficient way. This allows us to derive non-vacuous, numerically computable upper bounds on the generalization loss of the learned predictors after each task. We evaluate CoP2L on standard continual learning benchmarks under Class-Incremental and Task-Incremental settings, showing that it effectively mitigates catastrophic forgetting. It turns out that CoP2L is empirically competitive with baseline methods while certifying predictor reliability in continual learning with a non-vacuous bound.

1 INTRODUCTION

A common assumption in traditional machine learning is that the underlying data distribution does not evolve with time. In Continual Learning [De Lange et al., 2021, Wang et al., 2024], the goal is to develop machine learning algorithms that are able to learn under settings where this assumption is replaced by a setup where the model is trained on an evolving training data distribution, in such a way that samples are revealed one task at a time. However, neural networks trained on evolving data distributions tend to forget earlier tasks, a phenomenon known as catastrophic forgetting [McCloskey and Cohen, 1989, French, 1999, Goodfellow et al., 2014]. In order to cope with forgetting, various methodologies have been developed, such as regularization-based approaches [Kirkpatrick et al., 2017, Zenke et al., 2017, Li and Hoiem, 2017, Aljundi et al., 2018],



(a) Class-incremental setting



(b) Task-incremental setting

Figure 1: Numerical values of the proposed generalization bounds for continual learning over 10 tasks on CIFAR100, using ViT and ResNet50 backbones. The bounds hold simultaneously for all tasks.

architectural-based approaches [Rusu et al., 2016, Mallya et al., 2018, Aljundi et al., 2017, Mallya and Lazebnik, 2018, Wang et al., 2022, He et al., 2025, Gao et al., 2023, Zhou et al., 2025, 2024] or rehearsal-based approaches [Rolnick et al., 2019, Chaudhry et al., 2019, Shin et al., 2017, Rebuffi et al., 2017a, Buzzega et al., 2020].

We develop a novel sample compression theory for continual learning. Being agnostic to the architecture, our theoretic

cal results are well-suited for rehearsal-based approaches, which are commonly used in the continual learning literature for practical applications [Libera et al., 2023, Mai et al., 2020, Chaudhry et al., 2019, Aljundi et al., 2019]. We then propose a theoretically motivated algorithm that uses the replay buffer only when necessary to mitigate the forgetting. These new results pave the way for continual learning approaches based on theoretical guarantees.

More precisely, our proposed continual learning scheme builds upon the Pick-to-Learn meta-algorithm (P2L) of Paccagnan et al. [2024]. This meta-algorithm was developed specifically with sample compression theory in mind [Floyd and Warmuth, 1995, Campi and Garatti, 2023]. By finding a small subset of the data such that a predictor learned on this subset achieves low error on the whole training set, P2L enables computing tight upper bounds for the generalization error of the learned predictor. This ability of a learning algorithm to simultaneously output a predictor and its risk certificate has been coined as *self-certified learning* [Freund, 1998, Pérez-Ortiz et al., 2021, Marks and Paccagnan, 2025]. This certification is arguably an asset to increase the *trustworthiness* of machine learning systems.

The *Continual Pick-to-Learn* (CoP2L)¹ algorithm that we propose leverages sample compression theory to intelligently select the training data from earlier tasks to mitigate forgetting. We derive high-confidence upper bounds on the generalization error for each task simultaneously, estimated directly from the training set. We also empirically show that CoP2L substantially mitigates forgetting and is comparable with several standard baselines. Our contributions can be summarized as follows:

- (1) We propose the algorithm *Continual Pick-to-Learn* (CoP2L), that integrates the sample compression theory within the continual learning setup. To the best of our knowledge, we are the first to integrate the theoretical results from sample compression to rehearsal-based continual learning.
- (2) CoP2L is able to provide high confidence non-trivial upper bounds for the generalization error by means of the sample compression theory. We experimentally showcase that the bounds are numerically computable, have non-trivial values and follow the general error trends observed on the test set. Therefore, they can actually be used as risk certificates for the model’s behaviour on the learned tasks, improving the trustworthiness of the continually learnt model.
- (3) We experimentally show with a wide range of experiments that CoP2L significantly mitigates forgetting, while also being able to obtain comparable performance compared with several strong continual learning baselines.

¹Our code is available at https://anonymous.4open.science/r/CoP2L_paper_code-0058/

1.1 RELATED WORK

Continual learning approaches. In the continual learning literature, various practical approaches have been developed to mitigate forgetting. Broadly, the approaches could be divided into three categories: 1) regularization-based approaches [Kirkpatrick et al., 2017, Zenke et al., 2017, Li and Hoiem, 2017, Aljundi et al., 2018], 2) architecture-based approaches [Rusu et al., 2016, Mallya et al., 2018, Aljundi et al., 2017, Mallya and Lazebnik, 2018, Wang et al., 2022, He et al., 2025, Gao et al., 2023, Zhou et al., 2025, 2024] and 3) rehearsal-based approaches [Rolnick et al., 2019, Chaudhry et al., 2019, Shin et al., 2017, Rebuffi et al., 2017a, Buzzega et al., 2020].

Most rehearsal-based approaches use a *replay buffer* that contains a small subset of the dataset over which the model continues to train, even when learning over new tasks. The buffer helps to mitigate the forgetting of a model on previous tasks. However, the effect of the buffer depends on the quality of the data chosen in the buffer. A naive approach is to sample randomly the datapoints [Mai et al., 2020, Libera et al., 2023]. Non-naive methods include methods such as iCarl [Rebuffi et al., 2017a], Dark Experience Replay [Buzzega et al., 2020], Gradient Episodic Memory [Lopez-Paz and Ranzato, 2017], Example Forgetting [Benkő, 2024], Global Pseudo-Task simulation [Liu et al., 2022] and Coreset-based methods [e.g., Hao et al., 2023, Tong et al., 2025, Borsos et al., 2020, Yoon et al., 2022].

Continual learning generalization bounds. In recent years, generalization bounds were proposed to study the asymptotic behavior of various specific models, e.g., for linear models [Evron et al., 2022, Goldfarb and Hand, 2023, Lin et al., 2023, Banayeeanzade et al., 2025]; for Neural Tangent Kernel models trained with Orthogonal Gradient Descent [Bennani and Sugiyama, 2020, Doan et al., 2021, Farajtabar et al., 2020]; for regularization-based methods [Yin et al., 2020]; or for a PackNet-inspired [Mallya and Lazebnik, 2018] model for continual representation learning [Li et al., 2022]. Learning algorithms with sample complexity guarantees were also proposed under data assumptions, such that all target tasks lie in a same space obtainable from a (linear or non-linear) combination of some input features [Cao et al., 2022]. Finally, Friedman and Meir [2025] presented new PAC-Bayes bounds for the backward transfer loss of stochastic models trained without a replay buffer.

In contrast with the listed works above, in this paper, we simultaneously provide risk certificates on the true risk of each task, our bound is non-asymptotic and can be computed from the training set. Moreover, our bound is applicable to any neural network architecture, under minimal data assumptions and does not have limitations on the continual learning setup that is employed.

Sample compression. The sample compression theory has been shown to be effective for providing tight generalization bounds [Marchand and Shawe-Taylor, 2002, Marchand and Sokolova, 2005, Laviolette et al., 2005, Campi and Garatti, 2023]. However, most sample compression approaches are limited to low-complexity models. A notable exception is the method Pick-to-Learn (P2L), presented by Paccagnan et al. [2024], which successfully provides guarantees for deep neural networks [Bazin et al., 2025] and Gaussian Processes [Marks and Paccagnan, 2025]. In this paper, we adapt the key ideas introduced in the sample compression theory to the continual learning case, which enables us to provide an upper bound on the true risk from training samples.

2 BACKGROUND

Continual learning. Let us consider a meta-distribution \mathcal{D} and a sequence of *i.i.d.* (independent and identically distributed) task distributions $\mathcal{D}_1, \mathcal{D}_2, \dots, \mathcal{D}_T \sim \mathcal{D}$ on an input-output space $\mathcal{X} \times \mathcal{Y}$. We are given a predictive *model* $f_\theta : \mathcal{X} \rightarrow \mathcal{Y}$ (e.g., a neural network architecture), with *learnable* parameters $\theta \in \Theta$. From randomly initialized parameters θ_0 , the aim of the continual learning process at step $t \in \{1, \dots, T\}$ is to update the parameters θ_{t-1} into θ_t by learning from a new task sample $S_t \sim \mathcal{D}_t$. We denote the training set at task t as $S_t = \{(\mathbf{x}_{t,i}, y_{t,i})\}_{i=1}^{n_t}$, with $\mathbf{x}_{t,i} \in \mathcal{X}$ and $y_{t,i} \in \mathcal{Y}_t \subseteq \mathcal{Y}$; that is, the same input space \mathcal{X} is shared among all tasks, and the output space \mathcal{Y} may be the union of several task specific output spaces \mathcal{Y}_t . Given a loss function $\ell : \Theta \times \mathcal{X} \times \mathcal{Y} \rightarrow [0, 1]$, we want the last updated predictor f_{θ_T} to maintain a low generalization loss on all observed tasks $t \in \{1, \dots, T\}$:

$$\mathcal{L}_{\mathcal{D}_t}(\theta_T) := \mathbf{E}_{(\mathbf{x}, y) \sim \mathcal{D}_t} \ell(\theta_T, \mathbf{x}, y). \quad (1)$$

The empirical loss counterpart on observed training samples is given by

$$\widehat{\mathcal{L}}_{S_t}(\theta_T) := \frac{1}{n_t} \sum_{i=1}^{n_t} \ell(\theta_T, \mathbf{x}_{t,i}, y_{t,i}). \quad (2)$$

The challenge of continual learning lies in the fact that the learner observes the task datasets $S_1, S_2, \dots, S_t, \dots, S_T$ sequentially and that we assume that the system cannot keep all observed data in memory. Nevertheless, at task t , we would like the system to perform well on all tasks, including the previous ones $1, \dots, t-1$. However, simply updating the parameters θ_{t-1} learned from a previous tasks to optimize the loss $\widehat{\mathcal{L}}_{S_t}(\theta_t)$ on a current task t would lead to *catastrophic forgetting* [French, 1999]. Therefore, as indicated in Section 1.1, numerous empirical methods have been developed to mitigate forgetting. A simple yet very effective strategy is to simply store a small subset of data from the earlier tasks, coined as the *replay buffer*, and to include them

in the objective function of the *experience replay* strategy for learning task t :

$$\mathcal{F}_t^{\text{replay}}(\theta_t) := \widehat{\mathcal{L}}_{S_t}(\theta_t) + \frac{1}{|\mathcal{B}|} \sum_{j \in \mathcal{B}} \ell(\theta_t, \mathbf{x}_j, y_j), \quad (3)$$

where the second term is the loss on the replay buffer \mathcal{B} .

Sample compression theory. Let us consider a training dataset $S = \{(\mathbf{x}_i, y_i)\}_{i=1}^n \in (\mathcal{X} \times \mathcal{Y})^n$ sampled *i.i.d.* from an unknown distribution \mathcal{D} , a family of learnable parameters Θ and a learning algorithm A such that $A(S) \in \Theta$. In this setting, sample compression theory provides generalization bounds for any predictor f_θ , with $\theta = A(S)$, on the condition that f_θ can be provably represented as a function of a small subset of the training dataset S , called the compression set, and an additional source of information, called the message. If this is the case, we call f_θ a sample-compressed predictor.

The compression set is denoted $S^{\mathbf{i}}$ and is parameterized by a strictly increasing sequence of indices $\mathbf{i} \in \mathcal{P}(n)$, with $\mathcal{P}(n)$ the powerset of $\{1, \dots, n\}$. The compression set is defined such that $S^{\mathbf{i}} = S^{(i_1, \dots, i_{|\mathbf{i}|})} = \{(\mathbf{x}_{i_1}, y_{i_1}), \dots, (\mathbf{x}_{i_{|\mathbf{i}|}}, y_{i_{|\mathbf{i}|}})\} \subseteq S$. We define the complement sequence \mathbf{i}^c such that $\mathbf{i} \cap \mathbf{i}^c = \emptyset$ and $\mathbf{i} \cup \mathbf{i}^c = \{1, \dots, n\}$. Thus, we have the complement set $S^{\mathbf{i}^c} = S \setminus S^{\mathbf{i}}$ and $|\mathbf{i}^c| = n - |\mathbf{i}|$.

In addition to the compression set, a message μ could be needed to compress the predictor. Although generally defined as a binary sequence, the message set can be any set of countable sequences of symbols. Let $\Sigma = \{\sigma_1, \sigma_2, \dots, \sigma_N\}$ be the alphabet used to construct the messages and Σ^* be the set of all possible sequences, of length 0 to ∞ , constructed using the alphabet Σ . For all $\mathbf{i} \in \mathcal{P}(n)$, we choose $\mathcal{M}(\mathbf{i})$ a countable subset of Σ^* , which represents all the possible messages that can be chosen for \mathbf{i} .

Given learned parameters $\theta = A(S)$, to prove that the predictor f_θ is a sample-compressed one, we need to define two functions: a compression function and a reconstruction function. The compression function $\mathcal{C} : \cup_{1 \leq n \leq \infty} (\mathcal{X} \times \mathcal{Y})^n \rightarrow \cup_{m \leq n} (\mathcal{X} \times \mathcal{Y})^m \times \cup_{\mathbf{i} \in \mathcal{P}(n)} \mathcal{M}(\mathbf{i})$ outputs a compression set $S^{\mathbf{i}}$ and a message μ . Then, the reconstruction function $\mathcal{R} : \cup_{m \leq n} (\mathcal{X} \times \mathcal{Y})^m \times \cup_{\mathbf{i} \in \mathcal{P}(n)} \mathcal{M}(\mathbf{i}) \rightarrow \Theta$ is defined such that $A(S) = \mathcal{R}(S^{\mathbf{i}}, \mu)$. The forthcoming results rely on a probability distribution over the set of sample-compressed predictors $\bar{\Theta} \subseteq \Theta$. For any sample-compressed predictor $\mathcal{R}(S^{\mathbf{i}}, \mu)$, this data-independent distribution is expressed as $P_{\bar{\Theta}}(\mathcal{R}(S^{\mathbf{i}}, \mu)) = P_{\mathcal{P}(n)}(\mathbf{i}) P_{\mathcal{M}(\mathbf{i})}(\mu)$, with $P_{\mathcal{P}(n)}$ a probability distribution over $\mathcal{P}(n)$ and $P_{\mathcal{M}(\mathbf{i})}$ a probability distribution over $\mathcal{M}(\mathbf{i})$. Following common practices [Marchand and Sokolova, 2005, Bazinet et al., 2025], we consider hereunder $P_{\mathcal{P}(n)}(\mathbf{i}) = \binom{n}{|\mathbf{i}|}^{-1} \zeta(|\mathbf{i}|)$, with $\zeta(k) = \frac{6}{\pi^2} (k+1)^{-2}$. Also, given a sequence of indices \mathbf{i} , we set $P_{\mathcal{M}(\mathbf{i})}$ to a uniform distribution over the messages.

We now present a recent generalization guarantee for sample compression [Bazinet et al., 2025], on which we build our theoretical framework. We use the shorthand notation $\widehat{\mathcal{L}}_S^{\text{ic}}(\cdot)$ to denote the empirical loss on the training sample that do not belong to the compression set: $S^{\text{ic}} = S \setminus S^{\text{i}}$; it is mandatory to use $\widehat{\mathcal{L}}_S^{\text{ic}}(\cdot)$ to obtain an unbiased estimate of the loss, as the predictor $\mathcal{R}(S^{\text{i}}, \mu)$ relies on S^{i} and the result wouldn't hold otherwise.

Theorem 2.1 (Bazinet et al., 2025). *For any distribution \mathcal{D} over $\mathcal{X} \times \mathcal{Y}$, for any family of set of messages $\{\mathcal{M}(\mathbf{i}) \mid \mathbf{i} \in \mathcal{P}(n)\}$, for any deterministic reconstruction function \mathcal{R} and for any $\delta \in (0, 1]$, with probability at least $1 - \delta$ over the draw of $S \sim \mathcal{D}^n$, we have*

$$\forall \mathbf{i} \in \mathcal{P}(n), \mu \in \mathcal{M}(\mathbf{i}) :$$

$$\mathcal{L}_{\mathcal{D}}(\theta_{\mathbf{i}, \mu}) \leq \text{kl}^{-1} \left(\widehat{\mathcal{L}}_S^{\text{ic}}(\theta_{\mathbf{i}, \mu}), \frac{1}{|\mathbf{i}^{\text{c}}|} \ln \frac{2 \binom{n}{|\mathbf{i}|} \sqrt{|\mathbf{i}^{\text{c}}|}}{\zeta(|\mathbf{i}|) P_{\mathcal{M}(\mathbf{i})}(\mu) \delta} \right),$$

with $\theta_{\mathbf{i}, \mu} = \mathcal{R}(S^{\text{i}}, \mu)$ the reconstructed parameters, $\text{kl}(q, p) = q \ln \frac{q}{p} + (1 - q) \ln \frac{1 - q}{1 - p}$ the binary Kullback-Leibler divergence and its inverse

$$\text{kl}^{-1}(q, \varepsilon) = \arg \sup_{p \in [0, 1]} \{\text{kl}(q, p) \leq \varepsilon\}. \quad (4)$$

On the one hand, given a fixed compression set size $|\mathbf{i}|$, the bound decreases when the training set size n increases. On the other hand, given a fixed dataset size n , the bound increases with $|\mathbf{i}|$.

Pick-to-Learn. To obtain sample compression guarantees for a class of predictors, it is necessary to prove that the learned predictor only depends on a small subset of the data and (optionally) a message. Some predictors, such as the SVM [Boser et al., 1992] and the perceptron [Rosenblatt, 1958, Moran et al., 2020], have a straightforward compression scheme, as they only depend on a subset of the data after training. Some learning algorithms, such as the set covering machine (SCM) [Marchand and Shawe-Taylor, 2002, Marchand et al., 2003, Marchand and Sokolova, 2005] and decision trees [Shah, 2007], necessitate hand-crafted compression schemes involving a message. Up until recently, there was no sample compression scheme for deep neural networks.

The meta-algorithm Pick-To-Learn (P2L) was proposed by Paccagnan et al. [2024] as a compression scheme for any class of predictors, with a specific focus on deep neural networks. The meta-algorithm acts as an additional training loop, by iteratively selecting datapoints over which the model is updated. Starting with initial parameters θ_{init} , P2L evaluates the predictor on the whole training dataset, adds the datapoints with the highest losses to the compression set and then updates the predictor using the compression set. The meta-algorithm stops once the losses of training points

Algorithm 1 Pick-To-Learn (P2L) [Paccagnan et al., 2024]

```

input  $\theta_{\text{init}}$                                 {Initial parameters of the model  $f_{\theta}$ }
input  $S = \{(\mathbf{x}_i, y_i)\}_{i=1}^n$                 {Training set}
input  $\gamma$                                        {Stopping criteria}
1:  $k \leftarrow 0; C_0 \leftarrow \emptyset; \theta_0 \leftarrow \theta_{\text{init}}$ 
2:  $(\bar{\mathbf{x}}, \bar{y}) \leftarrow \arg \max_{(\mathbf{x}, y) \in S} \ell(\theta_0, \mathbf{x}, y)$ 
3: while  $\ell(\theta_k, \bar{\mathbf{x}}, \bar{y}) \geq \gamma$  do
4:    $k \leftarrow k + 1$ 
5:    $C_k \leftarrow C_{k-1} \cup \{(\bar{\mathbf{x}}, \bar{y})\}$ 
6:    $\theta_k \leftarrow \mathbf{update}(\theta_{k-1}, C_k)$ 
7:    $(\bar{\mathbf{x}}, \bar{y}) \leftarrow \arg \max_{(\mathbf{x}, y) \in S \setminus C_k} \ell(\theta_k, \mathbf{x}, y)$ 
8: end while
9: return  $\theta_k$                                 {Final parameters}

```

that do not belong to the compression set are lower than a given stopping criterion γ . We provide the pseudo-code of P2L in Algorithm 1. Recent works introduce improvements to the original scheme, notably early stopping strategies [Bazinet et al., 2025, Paccagnan et al., 2025] and extension to the Bayesian setting [Marks and Paccagnan, 2025].

3 SAMPLE COMPRESSION FOR CONTINUAL LEARNING

A striking realization coming from the P2L algorithm is that only a small fraction of the training set – the compression set – needs to be provided to the learner in order to achieve good generalization. The winning strategy is to select this compression set to ensure a low risk on the training samples not being retained in the compression set (i.e., the complement of the compression set). This observation motivates the strategy employed in our new algorithm Continual Pick-To-Learn (CoP2L), which manages the *replay buffer* by subsampling only from the complement set instead of the whole training set. Then, while learning subsequent tasks, CoP2L maintains a low risk on previous tasks by adding well-chosen datapoints from the buffer to its compression set. This strategy inherently both mitigates the forgetting and enables the computation of sample compression bounds.

In CoP2L, each new task is learned by a modified version of the P2L meta-algorithm (Algorithm 2, entitled mP2L), as explained further down. That is, for each new task, the proposed continual learning algorithm (Algorithm 3) calls mP2L and then updates the replay buffer by sampling datapoints that were not chosen in the compression set. Similar to the replay buffer method, at the end of each task t , the buffer contains $\lfloor \frac{m}{t} \rfloor$ datapoints of each previous task, with m the maximum buffer size.

We modified Pick-To-Learn in two significant ways. **(i)** First, we introduced weights to the loss functions to tackle the imbalance problem between the current task and the previous tasks. Traditionally, when working with a replay buffer, the class imbalance problem is taken care of by training on a number of datapoints from previous tasks. As our model

Algorithm 2 Modified Pick-To-Learn (mP2L)

input θ_{init} {Initial parameters of the model f_θ }
input $S = \{(\mathbf{x}_i, y_i, w_i)\}_{i=1}^n$ {Training set (with weights)}
input $B^* = \{(\mathbf{x}_i, y_i, w_i)\}_{i=1}^m$ {Buffer set (with weights)}
input γ {Stopping criteria}
input K^* {Maximum number of iterations}

- 1: $k \leftarrow 0; C_0 \leftarrow \emptyset; \theta_0 \leftarrow \theta_{\text{init}}$
- 2: $S^* \leftarrow S \cup B^*$
- 3: $(\bar{\mathbf{x}}, \bar{y}, \bar{w}) \leftarrow \operatorname{argmax}_{(\mathbf{x}, y, w) \in S^*} \ell(\theta_0, \mathbf{x}, y) \cdot w$
- 4: **while** $\ell(\theta_k, \bar{\mathbf{x}}, \bar{y}) \cdot \bar{w} \geq \gamma$ and $k \leq K^*$ **do**
- 5: $k \leftarrow k + 1$
- 6: $C_k \leftarrow C_{k-1} \cup \{(\bar{\mathbf{x}}, \bar{y}, \bar{w})\}$
- 7: $\theta_k \leftarrow \mathbf{update}(\theta_{k-1}, C_k)$
- 8: $(\bar{\mathbf{x}}, \bar{y}, \bar{w}) \leftarrow \operatorname{argmax}_{(\mathbf{x}, y, w) \in S^* \setminus C_k} \ell(\theta_k, \mathbf{x}, y) \cdot w$
- 9: **end while**
- 10: **if** $k < K^*$ **then**
- 11: $k \leftarrow \operatorname{argmin}_{0 \leq k' \leq k} \Psi(S, \theta_{k'}, C_{k'} \cap S)$ {Eq. (5)}
- 12: **end if**
- 13: **return** θ_k, C_k {Final parameters and compression set}

is only trained on a very limited subset of the data, another strategy must be implemented to mitigate the class imbalance effect. Before starting the training on a new task, mP2L sets the weight of the datapoints from the previous task to $\omega > 1$ and the weight of the current task to 1. For the stopping criteria of mP2L to be satisfied, the worst loss on the current task must be less than γ and the worst loss on the previous tasks must be less than $\frac{\gamma}{\omega}$. (ii) The original P2L algorithm trains the model until it first achieves zero errors on the complement set. Instead, mP2L performs early stopping based on the bound value [as proposed by Bazinet et al., 2025]. That is, mP2L relies on the trade-off encoded in Theorem 2.1 between the accuracy on the complement set C and the complexity of the model f_θ . More precisely, it returns the model’s parameters θ that minimizes

$$\Psi(S, \theta, C) = \text{kl}^{-1} \left(\hat{\mathcal{L}}_{S \setminus C}(\theta), \frac{1}{|S \setminus C|} \ln \frac{2\sqrt{|S \setminus C|} \binom{|S|}{|C|}}{\zeta(|C|)\delta} \right), \quad (5)$$

with kl^{-1} given by Eq. (4). Thanks to Theorem 2.1, we have that $\mathcal{L}_{\mathcal{D}}(\theta) \leq \Psi(S, \theta, C)$ with high probability.

Note that for the first observed task, the mP2L procedure starts from randomly initialized parameters θ_0 and is executed on the training sample S_1 (as it is done by the original P2L). Then, for every subsequent task $t \in \{2, \dots, T\}$, the mP2L procedure is initialized to the previously learned parameters θ_{t-1} . It then learns from the current task sample S_t and a subset of randomly selected instances from previous tasks. The latter is obtained from the procedure **sample**(S, m) (see Algorithm 3), which represents the random sampling of m instances of S without replacement.²

²Although we only discuss random sampling, any buffer management technique applied to the complement set would be valid in CoP2L, such as coreset methods.

Algorithm 3 Continual Pick-To-Learn (CoP2L)

input θ_0 {Initial parameters of the model}
input S_1, S_2, \dots, S_T {Training sets}
input γ {mP2L’s stopping criteria}
input m {Buffer’s max sampling size}
input ω {Weight for buffer tasks}

- 1: $B_i \leftarrow \emptyset \quad \forall i = 1, \dots, T$
- 2: $B^* \leftarrow \emptyset$
- 3: **for** $t \in \{1, \dots, T\}$ **do**
- 4: $\hat{S}_t \leftarrow \{(\mathbf{x}, y, 1)\}_{(\mathbf{x}, y) \in S_t}$
- 5: $\theta_t, C^* \leftarrow \mathbf{mP2L}(\theta_{t-1}, \hat{S}_t, B^*, \gamma, \infty)$
- 6: $B_i \leftarrow \mathbf{sample}(B_i, \lfloor \frac{m}{t} \rfloor) \quad \forall i = 1, \dots, t-1$
- 7: $B_t \leftarrow \mathbf{sample}(\hat{S}_t \setminus C^*, \lfloor \frac{m}{t} \rfloor)$
- 8: $B^* \leftarrow \bigcup_{i=1}^t \{(\mathbf{x}, y, \omega)\}_{(\mathbf{x}, y, \cdot) \in B_i}$
- 9: **end for**
- 10: **return** θ_T . {Final parameters}

Compression and reconstruction scheme. From a theoretical standpoint, in contrast to the original P2L, both mP2L and CoP2L cannot be reconstructed straightforwardly without a message for two reasons: (1) when only the compression set is given as input, the bound function $\Psi(S, \theta, C)$ used as stopping criteria in mP2L cannot be computed on the whole dataset; (2) the sampling procedure **sample**(S, m) in CoP2L cannot be reproduced in the reconstruction step. In Appendix B, we prove that CoP2L is a sample-compression algorithm by providing its compression and reconstruction functions, which subsequently gives rise to sample-compression bounds as presented in Theorem 3.1. Noteworthy, after learning on T tasks, the compression function provides two compression sets S^i and S^j , along with a message pair $\mu = (\mu_1, \mu_2)$. As explained further in the appendix, the use of two compression sets, along with the first part of the message $\mu_1 = [\mu_1^i]_{i=1}^T$, serves the proper treatment of the weighted buffer B^* , while the second part of the message $\mu_2 = [\mu_2^j]_{i=1}^T$ contains the number of iterations K^* to perform for each call to mP2L. The set of all possible message pairs is denoted as $\mathcal{M}_{1:T}(\mathbf{j}) = \{2, \dots, T\}^{|\mathbf{j}|} \times [\mathbf{x}_{t=1}^T \{1, \dots, n_t + |\mathcal{B}|\}]$.

Generalization bound. Given the compression and reconstruction function detailed in Appendix B, Theorem 2.1 can be used to obtain generalization bounds on the last learned task, which is done by mP2L to compute the bound Ψ . However, this bound holds for only one distribution of data. Therefore, it cannot be applied to bound the risks of the learned predictor on previous tasks seen by CoP2L.

The next Theorem 3.1 holds for any previously learned tasks. For a dataset $S_t \sim \mathcal{D}_t$, we denote the loss on the complement set of the joint set $S_t^i \cup S_t^j$ as $\hat{\mathcal{L}}_{S_t^i \cap S_t^j}(\theta)$. Moreover, we denote the reconstruction function of CoP2L as $\mathcal{R}_{1:T}(S_t^i, S_t^j, \mu \mid S_1, \dots, S_{t-1}, S_{t+1}, \dots, S_T)$. This formulation is important for the following theorem, as the reconstruction function for task t is *conditioned* on all datasets S_1 to S_T , with the exception of S_t .

Theorem 3.1. For any set of distributions $\{\mathcal{D}_t\}_{t=1}^T$ over $\mathcal{X} \times \mathcal{Y}$ sampled from \mathfrak{D} , and for any $\delta \in (0, 1]$, with probability at least $1 - \delta$ over the draw of $S_{t'} \sim \mathcal{D}_{t'}$, $t' = 1, \dots, T$, we have

$$\forall t \in \{1, \dots, T\}, \mathbf{i}, \mathbf{j} \in \mathcal{P}(n_t), \mu = (\mu_1, \mu_2) \in \mathcal{M}_{1:T}(\mathbf{j}) :$$

$$\mathcal{L}_{\mathcal{D}_t}(\theta_{\mathbf{i}, \mathbf{j}, \mu}^{(t)}) \leq \text{kl}^{-1} \left(\widehat{\mathcal{L}}_{S_t}^{\mathbf{i}^c \cap \mathbf{j}^c}(\theta_{\mathbf{i}, \mathbf{j}, \mu}^{(t)}), \frac{\epsilon(\mathbf{i}, \mathbf{j}, \mu)}{n_t - |\mathbf{i}| - |\mathbf{j}|} \right),$$

with $\theta_{\mathbf{i}, \mathbf{j}, \mu}^{(t)} = \mathcal{R}_{1:T}(S_t^{\mathbf{i}}, S_t^{\mathbf{j}}, \mu | S_1, \dots, S_{t-1}, S_{t+1}, \dots, S_T)$ the reconstructed parameters given by Algorithm 5 and

$$\epsilon(\mathbf{i}, \mathbf{j}, \mu) = \ln \left[\frac{T}{\delta} \binom{n_t}{|\mathbf{i}|} \binom{n_t - |\mathbf{i}|}{|\mathbf{j}|} \frac{(T-1)^{|\mathbf{j}|}}{\zeta(|\mathbf{i}|)\zeta(|\mathbf{j}|)} \prod_{i=1}^T \frac{1}{\zeta(\mu_2^i)} \right].$$

The proof is given in Section D. It first relies on a tighter version of Theorem 2.1, where the $2\sqrt{n - |\mathbf{i}|}$ term is removed and a second compression set is considered. This new result is tailored to the continual learning setting. For all tasks 1 through T , Theorem 3.1 encodes a tradeoff similar to Theorem 2.1 between the predictor accuracy and its complexity. Here, the predictor complexity is evaluated using the size of the compression sets \mathbf{i} and \mathbf{j} and the probability of choosing a message. The probability of the messages μ_1 and μ_2 are functions of the size of \mathbf{j} and the number of tasks. Indeed, the probability of μ_1 decays when $|\mathbf{j}|$ and T grow larger. Moreover, the probability of μ_2 depends on the size of the compression set outputted by mP2L at each task T . Thus, the larger the compression sets, the smaller the probability of both messages. In conclusion, the bound encodes the ability of a model to minimize the loss on the dataset whilst still keeping \mathbf{i} and \mathbf{j} small.

4 EXPERIMENTS

In this section, we present experiments with CoP2L to demonstrate the tightness of our new generalization bounds for continual learning in two different settings. Afterward, we compare CoP2L to established baseline approaches to show that although our algorithm was first designed to obtain tight generalization bounds, its performances are still very competitive with established continual learning schemes.

Datasets and continual learning settings. We carry out experiments on CIFAR10 [Krizhevsky, 2012], CIFAR100 [Krizhevsky, 2012] and TinyImageNet [mnousta and Ali, 2017]. We report results in Class-Incremental (CI) and Task-Incremental (TI) continual learning settings, as defined in the Avalanche framework [Carta et al., 2023].

Baselines. To assess the effectiveness of our proposed method CoP2L, we benchmark against several strong and widely adopted baselines across Class-Incremental and Task-Incremental learning settings.

For the Class-Incremental setting, we use the baselines Replay [Rolnick et al., 2019], Dark Experience Replay (DER) [Buzzega et al., 2020], iCaRL [Rebuffi et al., 2017b], GDumb [Prabhu et al., 2020], Contrastive Continual Learning via Importance Sampling (CCLIS) [Li et al., 2024] and Coreset Selection via Reducible Loss (CSReL) [Tong et al., 2025]

In the Task-Incremental setting, we report Replay, DER, LaMAML [Gupta et al., 2020], Learning without Forgetting (LwF) [Li and Hoiem, 2017], CCLIS and CSReL.

All the details about the experiments can be found in Section E, alongside supplementary Class Incremental experiments on MNIST [LeCun et al., 2010], FashionMNIST (FMNIST) [Xiao et al., 2017] and EMNIST [Cohen et al., 2017]. Moreover, we present Domain-Incremental (DI) experiments on PermutedMNIST [Goodfellow et al., 2014] and RotatedMNIST [Ben-David et al., 2010]. We report all the results in Appendix E.3, including the standard deviations and the training times for each method.

Accuracy and Forgetting. We denote $A(t, \theta_T)$ the accuracy obtained on a task t of a model f_{θ_T} trained on T tasks. We report the average accuracy over T tasks,

$$\bar{A}(\theta_T) = \frac{1}{T} \sum_{t=1}^T A(t, \theta_T),$$

and the average forgetting at task T ,

$$\bar{F}(T) = \frac{1}{T-1} \sum_{t=1}^{T-1} [A(t, \theta_t) - A(t, \theta_T)].$$

4.1 STUDY OF OUR GENERALIZATION BOUND

In Figures 2 and 3, we present our generalization bound on the true risk for each task for CIFAR10 with 5 tasks and CIFAR100 with 20 tasks. These bounds are presented for Vision Transformer (ViT) [Dosovitskiy et al., 2021] networks and ResNet50 (RN50) [He et al., 2016] networks trained with a buffer size of 2000 under both Class-Incremental and Task-Incremental settings. We present the details for the computation of the bound in Section B.

We observe that although the bounds are calculated exclusively on the training set, their values are non-vacuous and follow the test set error trends. CoP2L achieves particularly tight generalization bounds in the Task-Incremental setting, where forgetting is inherently reduced due to access to task identities and the use of a separate classifier head for each task. These conditions allow the model to better compress task-specific knowledge, leading to both stronger theoretical guarantees and improved empirical performance. We also observe that with the ViT backbone, the bounds are significantly tighter than those obtained with the ResNet50

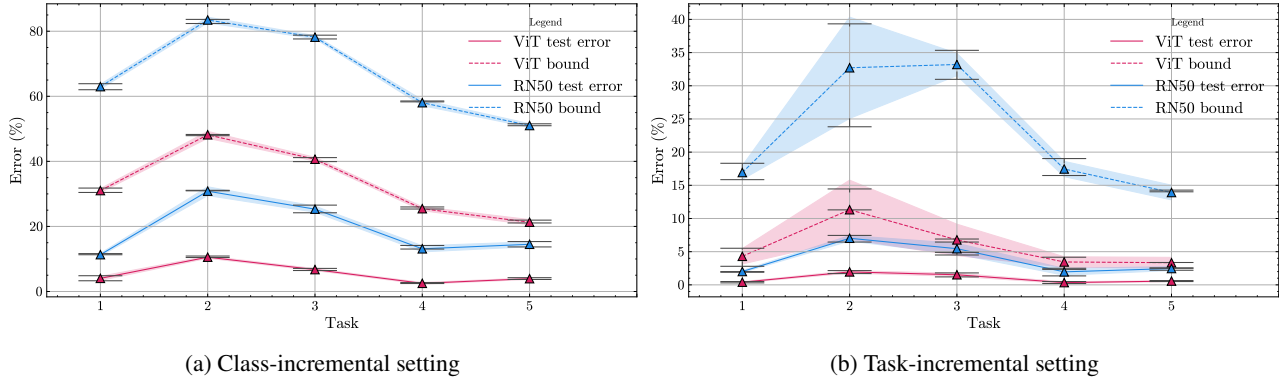


Figure 2: Illustration of the behavior of the bound on CIFAR10 with 5 tasks.

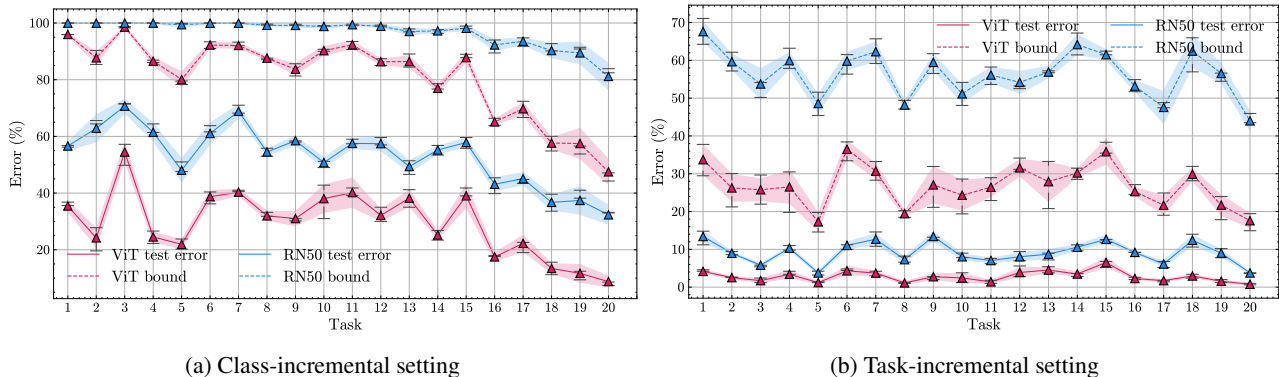


Figure 3: Illustration of the behavior of the bound on CIFAR100 with 20 tasks.

backbone. This is likely because the ViT backbone provides more structured and information-rich representations, which are easier to compress effectively, thereby enhancing the performance of CoP2L. Furthermore, the tightness of the bounds improves when the size of the dataset increases, which explains that the bounds on CIFAR10 (5000 samples per class) are noticeably tighter than the bounds on CIFAR100 (about 500 samples per class).

In addition, the complexity of the incremental scenario plays a role: CIFAR10 with 5 tasks involve learning two classes at a time, whereas CIFAR100 with 10 tasks require learning ten classes simultaneously, further contributing to looser bounds. Generalization bounds for multiple combinations of datasets and architectures are reported in Section E.4.

4.2 STUDY OF THE ALGORITHM'S PERFORMANCE

Table 1 presents results on CIFAR10, CIFAR100 and Tiny-ImageNet datasets, for both Class-Incremental and Task-Incremental settings. We observe that in Class-Incremental settings, CoP2L is competitive with most baselines in terms of accuracy while maintaining low forgetting. Alongside these baselines, we present results for finetuning a model

without a replay buffer, which evidently leads to a drastic drop in performance. In Task-Incremental settings, our method remains competitive. We note that even simple finetuning performs well in this setting. This behavior is expected, since adding a new classification head for each task naturally reduces forgetting. All the while being a competitive continual learning approach, CoP2L offers the additional advantage of certifying the generalization loss of the learned predictor. Further experiments on Imagenette and Imagewoof [Howard, 2019a] are presented in Appendix E. We do not present results for the ViT with CSReL, as the method is designed for small datasets (≈ 1000 datapoints), and becomes prohibitively more expensive when the dataset and the model grow in size. With the ResNet50, running CSReL was 5 to 32 times longer than executing CoP2L, while achieving much worse accuracy.

Finally, we refer the reader to Appendix F for an extended analysis of CoP2L behavior, including an ablation study on the loss terms, a sensitivity analysis with respect to task ordering, an analysis of the impact of buffer size, an ablation study on the use of early stopping with the bound and an evaluation of memory cost. Furthermore, we report experiments that CoP2L is able to mitigate forgetting more than the other methods while still retaining plasticity, and is able to achieve a balanced performance over past tasks.

Table 1: Summary of average accuracies and forgetting values obtained on various continual learning tasks on CIFAR10, CIFAR100 and TinyImageNet datasets.

(a) Class-Incremental experiments

Method	CIFAR10 (5 tasks)		CIFAR100 (10 tasks)		CIFAR100 (20 tasks)		TinyImNet (40 tasks)	
	Acc (\uparrow)	Forg (\downarrow)	Acc (\uparrow)	Forg (\downarrow)	Acc (\uparrow)	Forg (\downarrow)	Acc (\uparrow)	Forg (\downarrow)
CoP2L (ViT)	94.45	2.10	73.49	17.06	70.56	21.15	51.59	36.32
Finetuning (ViT)	27.55	89.74	12.87	93.27	8.49	94.64	2.83	95.36
Replay (ViT)	94.00	6.11	68.71	30.02	69.21	29.52	47.49	48.39
DER (ViT)	95.03	3.79	72.29	25.11	77.03	19.27	53.92	41.77
iCaRL (ViT)	88.60	3.13	65.54	13.64	62.36	15.88	21.06	34.49
GDumb (ViT)	94.16	3.16	72.51	11.53	72.35	11.77	53.93	15.11
CCLIS (ViT)	93.15	4.44	67.95	23.68	66.81	24.42	48.55	32.26
CoP2L (RN50)	80.98	5.84	49.53	22.31	46.74	22.54	33.30	35.93
Finetuning (RN50)	19.63	97.22	9.36	89.93	4.88	92.81	1.80	78.66
Replay (RN50)	81.38	17.72	49.41	42.12	49.44	44.96	28.38	63.36
DER (RN50)	82.35	15.31	49.37	44.01	57.53	33.37	28.77	64.17
iCaRL (RN50)	74.49	1.79	46.06	8.50	46.47	6.74	33.89	10.42
GDumb (RN50)	80.84	9.35	43.37	20.23	43.60	19.93	24.29	21.29
CCLIS (RN50)	76.89	12.32	44.22	23.23	39.10	25.78	18.32	40.40
CSReL (RN50)	34.50	26.44	38.75	42.12	32.57	40.23	12.84	73.69

(b) Task-Incremental experiments

Method	CIFAR10 (5 tasks)		CIFAR100 (10 tasks)		CIFAR100 (20 tasks)		TinyImNet (40 tasks)	
	Acc (\uparrow)	Forg (\downarrow)	Acc (\uparrow)	Forg (\downarrow)	Acc (\uparrow)	Forg (\downarrow)	Acc (\uparrow)	Forg (\downarrow)
CoP2L (ViT)	99.04	-0.00	95.03	0.90	97.18	0.56	93.81	1.50
Finetuning (ViT)	99.15	0.23	95.17	1.84	97.57	0.86	93.62	2.61
Replay (ViT)	99.29	-0.01	96.43	0.34	98.09	0.25	95.66	0.50
DER (ViT)	99.15	0.21	96.22	0.71	98.08	0.31	95.08	1.13
LaMAML (ViT)	99.25	0.05	95.58	0.58	97.84	0.26	94.82	0.79
LwF (ViT)	97.89	1.69	95.09	0.98	95.74	2.15	85.18	9.72
CCLIS (ViT)	98.81	0.48	90.99	4.49	94.86	2.88	86.82	6.14
CoP2L (RN50)	96.22	0.56	86.78	2.01	90.89	2.27	88.57	2.46
Finetuning (RN50)	96.60	1.00	88.23	1.78	93.25	1.27	90.62	1.38
Replay (RN50)	96.88	0.42	87.61	0.86	92.89	0.47	90.03	1.26
DER (RN50)	96.57	1.09	88.29	1.72	93.43	1.11	90.66	1.12
LaMAML (RN50)	96.65	0.73	83.57	6.18	89.89	4.12	87.20	4.53
LwF (RN50)	95.80	0.33	79.39	0.47	87.73	0.33	85.03	0.89
CCLIS (RN50)	95.45	0.79	78.55	6.76	83.51	6.60	75.65	14.12
CSReL (RN50)	65.46	13.66	69.14	15.17	63.52	14.49	50.22	22.34

5 CONCLUSION

We proposed CoP2L, an algorithm rooted in the sample compression theory, for self-certified continual learning. To the best of our knowledge, this is the first attempt to employ sample compression theory within the continual learning context. We provided sample compression bounds for CoP2L and verified empirically that they are non-vacuous and informative. We furthermore showed that on several

challenging datasets, our approach yields comparable results when compared to several strong baselines, while also providing learning guarantees for trustworthy continual learning. As the combination of Pick-to-Learn with experience replay leads to a successful learning scheme, we foresee that combining Pick-to-Learn with other continual learning approaches could lead to new compelling ways of obtaining self-certified predictors.

References

- Rahaf Aljundi, Punarjay Chakravarty, and Tinne Tuytelaars. Expert gate: Lifelong learning with a network of experts. In *2017 IEEE Conference on Computer Vision and Pattern Recognition, CVPR 2017, Honolulu, HI, USA, July 21-26, 2017*, 2017.
- Rahaf Aljundi, Francesca Babiloni, Mohamed Elhoseiny, Marcus Rohrbach, and Tinne Tuytelaars. Memory aware synapses: Learning what (not) to forget. In *European Conference on Computer Vision (ECCV)*, 2018.
- Rahaf Aljundi, Eugene Belilovsky, Tinne Tuytelaars, Laurent Charlin, Massimo Caccia, Min Lin, and Lucas Page-Caccia. Online continual learning with maximal interfered retrieval. In *Advances in Neural Information Processing Systems 32: Annual Conference on Neural Information Processing Systems 2019, NeurIPS 2019, December 8-14, 2019, Vancouver, BC, Canada*, 2019.
- Jason Ansel, Edward Yang, Horace He, Natalia Gimelshein, Animesh Jain, Michael Voznesensky, Bin Bao, Peter Bell, David Berard, Evgeni Burovski, Geeta Chauhan, Anjali Chourdia, Will Constable, Alban Desmaison, Zachary DeVito, Elias Ellison, Will Feng, Jiong Gong, Michael Gschwind, Brian Hirsh, Sherlock Huang, Kshiteej Kalam-barkar, Laurent Kirsch, Michael Lazos, Mario Lezcano, Yanbo Liang, Jason Liang, Yinghai Lu, CK Luk, Bert Maher, Yunjie Pan, Christian Puhrsch, Matthias Reso, Mark Saroufim, Marcos Yukio Siraichi, Helen Suk, Michael Suo, Phil Tillet, Eikan Wang, Xiaodong Wang, William Wen, Shunting Zhang, Xu Zhao, Keren Zhou, Richard Zou, Ajit Mathews, Gregory Chanan, Peng Wu, and Soumith Chintala. PyTorch 2: Faster Machine Learning Through Dynamic Python Bytecode Transformation and Graph Compilation. In *29th ACM International Conference on Architectural Support for Programming Languages and Operating Systems, Volume 2 (ASPLOS '24)*. ACM, 2024. doi: 10.1145/3620665.3640366.
- Mohammadamin Banayeeanzade, Mahdi Soltanolkotabi, and Mohammad Rostami. Theoretical insights into over-parameterized models in multi-task and replay-based continual learning. *Transactions on Machine Learning Research*, 2025. ISSN 2835-8856. URL <https://openreview.net/forum?id=4zGPT0ZwnU>.
- Mathieu Bazinet, Valentina Zantedeschi, and Pascal Germain. Sample compression unleashed: New generalization bounds for real valued losses. In *Proceedings of The 28th International Conference on Artificial Intelligence and Statistics*, Proceedings of Machine Learning Research, 2025.
- Shai Ben-David, John Blitzer, Koby Crammer, Alex Kulesza, Fernando Pereira, and Jennifer Wortman Vaughan. A theory of learning from different domains. *Machine learning*, 79(1):151–175, 2010.
- Beatrix Benkő. Example forgetting and rehearsal in continual learning. *Pattern Recognition Letters*, 2024.
- Mehdi Abbana Bennani and Masashi Sugiyama. Generalisation guarantees for continual learning with orthogonal gradient descent. *ArXiv preprint*, 2020.
- Zalán Borsos, Mojmir Mutny, and Andreas Krause. Core-sets via bilevel optimization for continual learning and streaming. In *Advances in Neural Information Processing Systems 33: Annual Conference on Neural Information Processing Systems 2020, NeurIPS 2020, December 6-12, 2020, virtual*, 2020.
- Bernhard E Boser, Isabelle M Guyon, and Vladimir N Vapnik. A training algorithm for optimal margin classifiers. In *Proceedings of the fifth annual workshop on Computational learning theory*, 1992.
- Pietro Buzzega, Matteo Boschini, Angelo Porrello, Davide Abati, and Simone Calderara. Dark experience for general continual learning: a strong, simple baseline. In *Advances in Neural Information Processing Systems 33: Annual Conference on Neural Information Processing Systems 2020, NeurIPS 2020, December 6-12, 2020, virtual*, 2020.
- Marco C Campi and Simone Garatti. Compression, generalization and learning. *Journal of Machine Learning Research*, 24(339):1–74, 2023.
- Xinyuan Cao, Weiyang Liu, and Santosh S. Vempala. Provable lifelong learning of representations. In *International Conference on Artificial Intelligence and Statistics, AISTATS 2022, 28-30 March 2022, Virtual Event*, Proceedings of Machine Learning Research, 2022.
- Mathilde Caron, Hugo Touvron, Ishan Misra, Hervé Jégou, Julien Mairal, Piotr Bojanowski, and Armand Joulin. Emerging properties in self-supervised vision transformers. In *Proceedings of the International Conference on Computer Vision (ICCV)*, 2021.
- Antonio Carta, Lorenzo Pellegrini, Andrea Cossu, Hamed Hemati, and Vincenzo Lomonaco. Avalanche: A pytorch library for deep continual learning. *Journal of Machine Learning Research*, 24(363):1–6, 2023. URL <http://jmlr.org/papers/v24/23-0130.html>.
- Arslan Chaudhry, Marc’Aurelio Ranzato, Marcus Rohrbach, and Mohamed Elhoseiny. Efficient lifelong learning with A-GEM. In *7th International Conference on Learning Representations, ICLR 2019, New Orleans, LA, USA, May 6-9, 2019*, 2019.
- Gregory Cohen, Saeed Afshar, Jonathan Tapson, and Andre Van Schaik. Emnist: Extending mnist to handwritten letters. In *2017 international joint conference on neural networks (IJCNN)*. IEEE, 2017.

- Matthias De Lange, Rahaf Aljundi, Marc Masana, Sarah Parisot, Xu Jia, Aleš Leonardis, Gregory Slabaugh, and Tinne Tuytelaars. A continual learning survey: Defying forgetting in classification tasks. *IEEE transactions on pattern analysis and machine intelligence*, 44(7):3366–3385, 2021.
- Jia Deng, Wei Dong, Richard Socher, Li-Jia Li, Kai Li, and Li Fei-Fei. Imagenet: A large-scale hierarchical image database. In *2009 IEEE conference on computer vision and pattern recognition*, pages 248–255. Ieee, 2009.
- Thang Doan, Mehdi Abbana Bennani, Bogdan Mazouze, Guillaume Rabusseau, and Pierre Alquier. A theoretical analysis of catastrophic forgetting through the NTK overlap matrix. In *The 24th International Conference on Artificial Intelligence and Statistics, AISTATS 2021, April 13-15, 2021, Virtual Event*, Proceedings of Machine Learning Research, 2021.
- Alexey Dosovitskiy, Lucas Beyer, Alexander Kolesnikov, Dirk Weissenborn, Xiaohua Zhai, Thomas Unterthiner, Mostafa Dehghani, Matthias Minderer, Georg Heigold, Sylvain Gelly, Jakob Uszkoreit, and Neil Houlsby. An image is worth 16x16 words: Transformers for image recognition at scale. In *International Conference on Learning Representations*, 2021.
- Itay Evron, Edward Moroshko, Rachel Ward, Nathan Srebro, and Daniel Soudry. How catastrophic can catastrophic forgetting be in linear regression? In *Conference on Learning Theory*. PMLR, 2022.
- Mehrdad Farajtabar, Navid Azizan, Alex Mott, and Ang Li. Orthogonal gradient descent for continual learning. In *The 23rd International Conference on Artificial Intelligence and Statistics, AISTATS 2020, 26-28 August 2020, Online [Palermo, Sicily, Italy]*, Proceedings of Machine Learning Research, 2020.
- Sally Floyd and Manfred Warmuth. Sample compression, learnability, and the vapnik-chervonenkis dimension. *Machine learning*, 21(3):269–304, 1995.
- Andrew YK Foong, Wessel P Bruinsma, and David R Burt. A note on the chernoff bound for random variables in the unit interval. *ArXiv preprint*, 2022.
- Robert M. French. Catastrophic forgetting in connectionist networks. *Trends in cognitive sciences*, 3(4):128–135, 1999.
- Yoav Freund. Self bounding learning algorithms. In *Proceedings of the Eleventh Annual Conference on Computational Learning Theory, COLT 1998, Madison, Wisconsin, USA, July 24-26, 1998*, 1998.
- Lior Friedman and Ron Meir. Data-dependent and oracle bounds on forgetting in continual learning. In *The 4th Conference on Lifelong Learning Agents*, 2025.
- Qiankun Gao, Chen Zhao, Yifan Sun, Teng Xi, Gang Zhang, Bernard Ghanem, and Jian Zhang. A unified continual learning framework with general parameter-efficient tuning. In *Proceedings of the IEEE/CVF International Conference on Computer Vision*, pages 11483–11493, 2023.
- Daniel Goldfarb and Paul Hand. Analysis of catastrophic forgetting for random orthogonal transformation tasks in the overparameterized regime. In *International Conference on Artificial Intelligence and Statistics*. PMLR, 2023.
- Ian J. Goodfellow, Mehdi Mirza, Da Xiao, Aaron Courville, and Yoshua Bengio. An empirical investigation of catastrophic forgetting in gradient-based neural networks. In *International Conference on Learning Representations (ICLR)*, 2014.
- Gunshi Gupta, Karmesh Yadav, and Liam Paull. Look-ahead meta learning for continual learning. In *Advances in Neural Information Processing Systems 33: Annual Conference on Neural Information Processing Systems 2020, NeurIPS 2020, December 6-12, 2020, virtual*, 2020.
- Jie Hao, Kaiyi Ji, and Mingrui Liu. Bilevel coreset selection in continual learning: A new formulation and algorithm. *Advances in Neural Information Processing Systems*, 2023.
- Charles R. Harris, K. Jarrod Millman, Stéfan J. van der Walt, Ralf Gommers, Pauli Virtanen, David Cournapeau, Eric Wieser, Julian Taylor, Sebastian Berg, Nathaniel J. Smith, Robert Kern, Matti Picus, Stephan Hoyer, Marten H. van Kerkwijk, Matthew Brett, Allan Haldane, Jaime Fernández del Río, Mark Wiebe, Pearu Peterson, Pierre Gérard-Marchant, Kevin Sheppard, Tyler Reddy, Warren Weckesser, Hameer Abbasi, Christoph Gohlke, and Travis E. Oliphant. Array programming with NumPy. *Nature*, 585(7825):357–362, 2020. doi: 10.1038/s41586-020-2649-2.
- Jiangpeng He, Zhihao Duan, and Fengqing Zhu. Cl-lora: Continual low-rank adaptation for rehearsal-free class-incremental learning. In *Proceedings of the Computer Vision and Pattern Recognition Conference*, pages 30534–30544, 2025.
- Kaiming He, Xiangyu Zhang, Shaoqing Ren, and Jian Sun. Deep residual learning for image recognition. In *2016 IEEE Conference on Computer Vision and Pattern Recognition, CVPR 2016, Las Vegas, NV, USA, June 27-30, 2016*, 2016.
- Jeremy Howard. Imagewoof: a subset of 10 classes from imagenet that aren’t so easy to classify, 2019a.
- Jeremy Howard. Imagenette: A smaller subset of 10 easily classified classes from imagenet, 2019b.

- Heechul Jung, Jeongwoo Ju, Minju Jung, and Junmo Kim. Less-forgetful learning for domain expansion in deep neural networks. In *Proceedings of the Thirty-Second AAAI Conference on Artificial Intelligence, (AAAI-18), the 30th innovative Applications of Artificial Intelligence (IAAI-18), and the 8th AAAI Symposium on Educational Advances in Artificial Intelligence (EAAI-18), New Orleans, Louisiana, USA, February 2-7, 2018*, 2018.
- James Kirkpatrick, Razvan Pascanu, Neil Rabinowitz, Joel Veness, Guillaume Desjardins, Andrei A Rusu, Kieran Milan, John Quan, Tiago Ramalho, Agnieszka Grabska-Barwinska, et al. Overcoming catastrophic forgetting in neural networks. *Proceedings of the national academy of sciences*, 114(13):3521–3526, 2017.
- Alex Krizhevsky. Learning multiple layers of features from tiny images. *University of Toronto*, 2012.
- John Langford. Tutorial on practical prediction theory for classification. *Journal of machine learning research*, 6(3), 2005.
- François Laviolette, Mario Marchand, and Mohak Shah. Margin-Sparsity Trade-Off for the Set Covering Machine. In *European Conference on Machine Learning*, pages 206–217. Springer, 2005.
- Yann LeCun, Léon Bottou, Yoshua Bengio, and Patrick Haffner. Gradient-based learning applied to document recognition. *Proceedings of the IEEE*, 86(11):2278–2324, 1998.
- Yann LeCun, Corinna Cortes, and CJ Burges. Mnist handwritten digit database. *ATT Labs*, 2010.
- Jiyong Li, Dilshod Azizov, Yang LI, and Shangsong Liang. Contrastive continual learning with importance sampling and prototype-instance relation distillation. *Proceedings of the AAAI Conference on Artificial Intelligence*, 38(12):13554–13562, 2024. doi: 10.1609/aaai.v38i12.29259. URL <https://ojs.aaai.org/index.php/AAAI/article/view/29259>.
- Yingcong Li, Mingchen Li, M. Salman Asif, and Samet Oymak. Provable and efficient continual representation learning. *ArXiv preprint*, 2022.
- Zhizhong Li and Derek Hoiem. Learning without forgetting. *IEEE transactions on pattern analysis and machine intelligence*, 40(12):2935–2947, 2017.
- Luca Della Libera, Pooneh Mousavi, Salah Zaiem, Cem Subakan, and Mirco Ravanelli. Cl-masr: A continual learning benchmark for multilingual asr. *IEEE/ACM Transactions on Audio, Speech, and Language Processing*, 2023.
- Sen Lin, Peizhong Ju, Yingbin Liang, and Ness Shroff. Theory on forgetting and generalization of continual learning. In *Proceedings of the 40th International Conference on Machine Learning*, Proceedings of Machine Learning Research, 2023.
- Yejia Liu, Wang Zhu, and Shaolei Ren. Navigating memory construction by global pseudo-task simulation for continual learning. *Advances in Neural Information Processing Systems*, 2022.
- David Lopez-Paz and Marc’Aurelio Ranzato. Gradient episodic memory for continual learning. In *Advances in Neural Information Processing Systems 30: Annual Conference on Neural Information Processing Systems 2017, December 4-9, 2017, Long Beach, CA, USA*, 2017.
- Zheda Mai, Hyunwoo J. Kim, Jihwan Jeong, and Scott Sanner. Batch-level experience replay with review for continual learning. *ArXiv preprint*, 2020.
- Arun Mallya and Svetlana Lazebnik. Packnet: Adding multiple tasks to a single network by iterative pruning. In *2018 IEEE Conference on Computer Vision and Pattern Recognition, CVPR 2018, Salt Lake City, UT, USA, June 18-22, 2018*, 2018.
- Arun Mallya, Dillon Davis, and Svetlana Lazebnik. Piggyback: Adapting a single network to multiple tasks by learning to mask weights. In *European Conference on Computer Vision (ECCV)*, 2018.
- Mario Marchand and John Shawe-Taylor. The set covering machine. *Journal of Machine Learning Research*, 3(Dec): 723–746, 2002.
- Mario Marchand and Marina Sokolova. Learning with decision lists of data-dependent features. *Journal of Machine Learning Research*, 6(4), 2005.
- Mario Marchand, Mohak Shah, John Shawe-Taylor, and Marina Sokolova. The set covering machine with data-dependent half-spaces. In *Machine Learning, Proceedings of the Twentieth International Conference (ICML 2003), August 21-24, 2003, Washington, DC, USA*, 2003.
- Daniel Marks and Dario Paccagnan. Pick-to-learn and self-certified gaussian process approximations. In *Proceedings of The 28th International Conference on Artificial Intelligence and Statistics*, Proceedings of Machine Learning Research, 2025.
- Michael McCloskey and Neal J. Cohen. Catastrophic interference in connectionist networks: The sequential learning problem. *Psychology of Learning and Motivation*, 1989.
- mnmostafa and Mohammed Ali. Tiny imagenet. <https://kaggle.com/competitions/tiny-imagenet>, 2017. Kaggle.

- Shay Moran, Ido Nachum, Itai Panasoff, and Amir Yehudayoff. On the perceptron’s compression. In *Beyond the Horizon of Computability: 16th Conference on Computability in Europe, CiE 2020, Fisciano, Italy, June 29–July 3, 2020, Proceedings 16*. Springer, 2020.
- Dario Paccagnan, Marco Campi, and Simone Garatti. The pick-to-learn algorithm: Empowering compression for tight generalization bounds and improved post-training performance. *Advances in Neural Information Processing Systems*, 2024.
- Dario Paccagnan, Daniel Marks, Marco C Campi, and Simone Garatti. Pick-to-learn for systems and control: Data-driven synthesis with state-of-the-art safety guarantees. *arXiv preprint arXiv:2512.04781*, 2025.
- María Pérez-Ortiz, Omar Rivasplata, John Shawe-Taylor, and Csaba Szepesvári. Tighter risk certificates for neural networks. *J. Mach. Learn. Res.*, 2021.
- Ameya Prabhu, Philip HS Torr, and Puneet K Dokania. Gdumb: A simple approach that questions our progress in continual learning. In *Computer Vision–ECCV 2020: 16th European Conference, Glasgow, UK, August 23–28, 2020, Proceedings, Part II 16*. Springer, 2020.
- Sylvestre-Alvise Rebuffi, Alexander Kolesnikov, Georg Sperl, and Christoph H. Lampert. icarl: Incremental classifier and representation learning. In *2017 IEEE Conference on Computer Vision and Pattern Recognition, CVPR 2017, Honolulu, HI, USA, July 21-26, 2017*, 2017a.
- Sylvestre-Alvise Rebuffi, Alexander Kolesnikov, Georg Sperl, and Christoph H. Lampert. icarl: Incremental classifier and representation learning. In *2017 IEEE Conference on Computer Vision and Pattern Recognition, CVPR 2017, Honolulu, HI, USA, July 21-26, 2017*, 2017b.
- David Rolnick, Arun Ahuja, Jonathan Schwarz, Timothy P. Lillicrap, and Gregory Wayne. Experience replay for continual learning. In *Advances in Neural Information Processing Systems 32: Annual Conference on Neural Information Processing Systems 2019, NeurIPS 2019, December 8-14, 2019, Vancouver, BC, Canada*, 2019.
- Frank Rosenblatt. The perceptron: a probabilistic model for information storage and organization in the brain. *Psychological review*, 65(6):386, 1958.
- Andrei A. Rusu, Neil C. Rabinowitz, Guillaume Desjardins, Hubert Soyer, James Kirkpatrick, Koray Kavukcuoglu, Razvan Pascanu, and Raia Hadsell. Progressive neural networks. *ArXiv preprint*, 2016.
- Mohak Shah. Sample compression bounds for decision trees. In *Machine Learning, Proceedings of the Twenty-Fourth International Conference (ICML 2007), Corvallis, Oregon, USA, June 20-24, 2007*, ACM International Conference Proceeding Series, 2007.
- Hanul Shin, Jung Kwon Lee, Jaehong Kim, and Jiwon Kim. Continual learning with deep generative replay. In *Advances in Neural Information Processing Systems 30: Annual Conference on Neural Information Processing Systems 2017, December 4-9, 2017, Long Beach, CA, USA*, 2017.
- Ruilin Tong, Yuhang Liu, Javen Qinfeng Shi, and Dong Gong. Coreset selection via reducible loss in continual learning. In *The Thirteenth International Conference on Learning Representations*, 2025.
- Paul Viallard, Pascal Germain, Amaury Habrard, and Emilie Morvant. Self-bounding majority vote learning algorithms by the direct minimization of a tight pac-bayesian c-bound. In *Machine Learning and Knowledge Discovery in Databases. Research Track: European Conference, ECML PKDD 2021, Bilbao, Spain, September 13–17, 2021, Proceedings, Part II 21*. Springer, 2021.
- Liyuan Wang, Xingxing Zhang, Hang Su, and Jun Zhu. A comprehensive survey of continual learning: Theory, method and application. *IEEE transactions on pattern analysis and machine intelligence*, 46(8):5362–5383, 2024.
- Zifeng Wang, Zizhao Zhang, Chen-Yu Lee, Han Zhang, Ruoxi Sun, Xiaoqi Ren, Guolong Su, Vincent Perot, Jennifer Dy, and Tomas Pfister. Learning to prompt for continual learning. In *IEEE/CVF Conference on Computer Vision and Pattern Recognition (CVPR)*, 2022.
- Han Xiao, Kashif Rasul, and Roland Vollgraf. Fashion-mnist: a novel image dataset for benchmarking machine learning algorithms, 2017.
- Dong Yin, Mehrdad Farajtabar, Ang Li, Nir Levine, and Alex Mott. Optimization and generalization of regularization-based continual learning: a loss approximation viewpoint. *ArXiv preprint*, 2020.
- Jaehong Yoon, Divyam Madaan, Eunho Yang, and Sung Ju Hwang. Online coreset selection for rehearsal-based continual learning. In *International Conference on Learning Representations*, 2022.
- Friedemann Zenke, Ben Poole, and Surya Ganguli. Continual learning through synaptic intelligence. In *Proceedings of the 34th International Conference on Machine Learning, ICML 2017, Sydney, NSW, Australia, 6-11 August 2017*, Proceedings of Machine Learning Research, 2017.
- Da-Wei Zhou, Hai-Long Sun, Han-Jia Ye, and De-Chuan Zhan. Expandable subspace ensemble for pre-trained model-based class-incremental learning. In *Proceedings of the IEEE/CVF Conference on Computer Vision and Pattern Recognition*, pages 23554–23564, 2024.

Da-Wei Zhou, Zi-Wen Cai, Han-Jia Ye, De-Chuan Zhan,
and Ziwei Liu. Revisiting class-incremental learning with
pre-trained models: Generalizability and adaptivity are
all you need. *International Journal of Computer Vision*,
133(3):1012–1032, 2025.

Sample Compression for Self-Certified Continual Learning: (Supplementary Materials)

Jacob Comeau^{1,2}

Mathieu Bazinet^{1,2}

Pascal Germain^{1,2}

Cem Subakan^{1,2,3}

¹Département d’informatique et génie logiciel, Université Laval, Québec, Qc, Canada

²Mila - Quebec Artificial Intelligence Institute , Montreal, Qc, Canada

³Computer Science and Software Engineering Department , Concordia University , Montreal, Qc, Canada

A TABLE OF SYMBOLS

We summarize the notation and their definitions in the following table.

Table 2: Summary table of the symbols used in this paper.

Symbol	Definition
\mathcal{X}	A feature space
\mathcal{Y}	A label space
S	A dataset composed of datapoints in $\mathcal{X} \times \mathcal{Y}$
\mathcal{D}	A distribution over $\mathcal{X} \times \mathcal{Y}$
\mathfrak{D}	A meta-distribution over the space of distributions \mathcal{D}
Θ	A set of learnable parameters θ
f_θ	A function $f_\theta : \mathcal{X} \rightarrow \mathcal{Y}$ parametrized by $\theta \in \Theta$
A	An learning algorithm that returns parameters $\theta \in \Theta$
\mathbf{i}	The indices of the compression set $S^{\mathbf{i}}$
\mathbf{i}^c	The indices of the compression set’s complement $S^{\mathbf{i}^c}$
$ \mathbf{i} $	The size of the compression set
\mathbf{j}	The indices of the second compression set $S^{\mathbf{j}}$ used by CoP2L
$\mathcal{P}(n)$	The powerset of $\{1, \dots, n\}$
μ	A message
Σ	The alphabet of symbols σ used to create the message μ
Σ^*	The set of all possible sequences of symbols $\sigma \in \Sigma$
$\mathcal{M}(\mathbf{i})$	The set of possible messages in Σ^* given a sequence \mathbf{i}
\mathcal{C}	The compression function
\mathcal{R}	The reconstruction function
Ψ	The sample-compression bound of Equation (5)
ℓ	A loss function $\ell : \Theta \times \mathcal{X} \times \mathcal{Y} \rightarrow [0, 1]$
$\widehat{\mathcal{L}}_S$	The empirical loss over a dataset S given a loss function ℓ
$\widehat{\mathcal{L}}_S^{\mathbf{i}}$	The empirical loss over a dataset $S^{\mathbf{i}}$ given a loss function ℓ
\mathcal{L}_D	The true loss over a distribution \mathcal{D} given a loss function ℓ

B COMPRESSION AND RECONSTRUCTION FUNCTIONS

In line with the prevalent literature, we introduced the sample compression framework based on a compression function providing a compression set and optionally a message. In the case of CoP2L, the reconstruction scheme relies on two compression sets (S^i, S^j) and a message pair (μ_1, μ_2) , which we explain later in this section.¹

Algorithm 4 Compression function of Continual Pick-To-Learn (CoP2L)

input θ_0	{Initialization parameters of the model}
input S_1, S_2, \dots, S_T	{Training sets}
input γ	{P2L's stopping criteria}
input m	{Buffer's max sampling size}
input ω	{Weight for buffer tasks}

```

1:  $B_t \leftarrow \emptyset, S_t^i \leftarrow \emptyset, S_t^j \leftarrow \emptyset, \mu_{1,t} \leftarrow \emptyset \quad \forall t = 1, \dots, T$ 
2:  $B^* \leftarrow \emptyset, \mu_2 \leftarrow \emptyset$ 
3: for  $t \in \{1, \dots, T\}$  do
4:    $\hat{S}_t \leftarrow \{(\mathbf{x}, y, 1)\}_{(\mathbf{x}, y) \in S_t}$ 
5:    $\theta_t, C^* \leftarrow \text{mP2L}(\theta_{t-1}, \hat{S}_t, B^*, \gamma, \infty)$ 
6:    $\mu_2^t \leftarrow |C^*|$ 
7:    $S_t^i \leftarrow S_t^i \cup (C^* \cap S_t) \quad \forall i = 1, \dots, t$ 
8:    $B_i \leftarrow \text{sample}(B_i, \lfloor \frac{m}{t} \rfloor) \quad \forall i = 1, \dots, t-1$ 
9:    $B_t \leftarrow \text{sample}(S_t \setminus C^*, \lfloor \frac{m}{t} \rfloor)$ 
10:  for  $i \in \{1, \dots, t-1\}$  do
11:    for  $(\mathbf{x}_{i,j}, y_{i,j}, \cdot) \in B^*$  and  $(\mathbf{x}_{i,j}, y_{i,j}, \cdot) \notin B_i$  do
12:       $S_i^j \leftarrow S_i^j \cup \{(\mathbf{x}_{i,j}, y_{i,j})\}$ 
13:       $S_i^i \leftarrow S_i^i \setminus \{(\mathbf{x}_{i,j}, y_{i,j})\}$ 
14:       $\mu_{1,i}^j \leftarrow \{t\}$ 
15:    end for
16:  end for
17:   $B^* \leftarrow \bigcup_{i=1}^t \{(\mathbf{x}, y, \omega)\}_{(\mathbf{x}, y, \cdot) \in B_i}$ 
18: end for
19: return  $\theta_T, \{S_t^i\}_{t=1}^T, \{S_t^j\}_{t=1}^T, \{\mu_{1,t}\}_{t=1}^T, \mu_2$ 

```

{Learned parameters, compression sets and message sets}

B.1 COMPRESSION FUNCTION

Two challenges prevent CoP2L (as presented by Algorithm 3) from being used as its own compression and reconstruction function, as it is done when working with the original P2L algorithm in a standard (non continual learning) setting. In this subsection, we expose each of these challenges while explaining how the proposed compression algorithm (Algorithm 4) allows to circumvent them.

The first challenge comes from the sampling of the buffer B^* (Lines 6 to 8 of Algorithm 3). When training using CoP2L, datapoints from the buffer can be chosen to be part of the compression set. At the next task, these datapoints may still be available to train the model (if they are not excluded from the buffer by the sampling step). Therefore, the reconstruction function needs to know when to remove the datapoint. The message μ_1 returned by Algorithm 4 thus provides the task index after which the datapoint was removed during the execution of CoP2L. As the reconstruction function only requires a message for datapoints who were removed from the buffer after being added to the compression set S^i , a second compression set S^j is dedicated to datapoints that necessitate a message. The message μ_1 given is chosen among $\{2, \dots, T\}$ for each datapoint belonging to S^j .

The second challenge is the use of the bound as stopping criterion in mP2L. Recall that the reconstruction function does not have access to the whole dataset. Thus, it cannot recover the bound value computed during the initial training phase (see Line 11 of Algorithm 2) and use it as a stopping criterion. To address this inconvenience, the number of iterations to perform is provided to mP2L as a message $\mu_2 = (\mu_2^1, \dots, \mu_2^T)$. That is, for each task t , with a buffer \mathcal{B} , the message component μ_2^t is chosen in $\{1, \dots, n_t + |\mathcal{B}|\}$, giving the number of mP2L's iterations to perform.

After learning on T tasks, the compression function provides the sample compression set S^i and S^j , along with a message

¹The idea of using multiple compression sets appeared in Marchand and Shawe-Taylor [2002] and Marchand et al. [2003], but in a setting without a message.

Algorithm 5 Reconstruction function of Continual Pick-To-Learn (CoP2L)

```
input  $\theta_0$  {Initialization parameters of the model}
input  $S_1^i, S_2^i, \dots, S_T^i$  {Compression sets}
input  $S_1^j, S_2^j, \dots, S_T^j$  {Compression sets}
input  $\mu_{1,1}, \mu_{1,2}, \dots, \mu_{1,T}$  {Message sets}
input  $\mu_2$  {Message set}
input  $\gamma$  {P2L's stopping criteria}
input  $m$  {Buffer's max sampling size}
input  $\omega$  {Weight for buffer tasks}
1:  $B^* \leftarrow \emptyset$ 
2: for  $t \in \{1, \dots, T\}$  do
3:  $\hat{S}_t \leftarrow \{(\mathbf{x}, y, 1)\}_{(\mathbf{x}, y) \in S_t^i}$ 
4:  $\theta_t, C^* \leftarrow \text{mP2L}(\theta_{t-1}, \hat{S}_t, B^*, \gamma, \mu_2^t)$ 
5:  $B_t \leftarrow (S_t^i \setminus C^*) \cup S_t^j$ 
6: for  $i \in \{1, \dots, t-1\}$  do
7:   for  $(\mathbf{x}_{i,j}, y_{i,j}, \omega_i) \in S_i^j$  do
8:     if  $\mu_{1,i}^j = t$  then
9:        $B_i \leftarrow B_i \setminus \{(\mathbf{x}_{i,j}, y_{i,j}, \omega_i)\}$ 
10:    end if
11:  end for
12:   $B^* \leftarrow \bigcup_{i=1}^t \{(\mathbf{x}, y, \omega)\}_{(\mathbf{x}, y, \cdot) \in B_i}$ 
13: end for
14: end for
15: return  $\theta_T$ . {Learned parameters}
```

pair (μ_1, μ_2) chosen among the set of all possible messages, denoted as

$$\mathcal{M}_{1:T}(\mathbf{j}) = \{2, \dots, T\}^{|\mathbf{j}|} \times \left[\prod_{t=1}^T \{1, \dots, n_t + |\mathcal{B}|\} \right]. \quad (6)$$

B.2 RECONSTRUCTION FUNCTION

Under the assumption that the input parameters $\theta_0, \gamma, m, \omega$ are the same for the compression function (Algorithm 4) and for CoP2L (Algorithm 3), the composition of the compression and the reconstruction function must output the exact same predictor as CoP2L. However, it only has access to the compression sets and the messages. The first challenge of the compression function is addressed using μ_1 from line 6 to 11 of Algorithm 5. For each datasets, we verify if a datapoint was previously excluded from the buffer by the sampling function. If so, we remove it from the buffer. The second challenge is addressed in line 4 of Algorithm 5 by giving the message μ_2 to mP2L as stopping criterion.

B.3 COMPUTATION OF THE BOUND

To compute the bound of Theorem 3.1, we need three things : the size of the first compression set \mathbf{i} , the size of the second compression set \mathbf{j} and the message μ . By simply running our CoP2L, we are able to retrieve $|\mathbf{i}| + |\mathbf{j}|$, but not the size of each compression set individually. Moreover, we are completely unable to retrieve the messages. Thus, instead of implementing Algorithm 3, we actually implemented the compression function as described in Algorithm 4.

Moreover, we use a block version of P2L, as defined by Algorithm 2 of Paccagnan et al. [2024]. We thus add k datapoints at once to the compression set at Line 6 of Algorithm 2 (the used values of k for each experiments is given in Section E.2. Thus, the value of μ_2^t (Line 6 of Algorithm 4) becomes the number of iterations of the mP2L algorithm at for task t . Knowing that mP2L outputs a compression set C_t^* , and adds k datapoints to the compression set at each iteration, the number of iterations is $\mu_2^t = \frac{|C_t^*|}{k}$. Finally, when computing the bound, we use the code provided by Viillard et al. [2021] to invert the kl divergence.

C TIGHTER SAMPLE COMPRESSION kl BOUND

In this section, we prove a tighter kl bound that is not derived from Theorem 2.1 but proved in a very similar way. To do so, we start by providing the Chernoff test-set bound for losses in $[0, 1]$ [Langford, 2005, Foong et al., 2022].

Theorem C.1 (Foong et al., 2022). *Let X_1, \dots, X_n be i.i.d. random variables with $X_i \in [0, 1]$ and $\mathbb{E}[X_i] = p$. Then, for any $\delta \in (0, 1]$, with probability at least $1 - \delta$*

$$p \leq \text{kl}^{-1}\left(\frac{1}{n} \sum_{i=1}^n X_i, \frac{1}{n} \ln \frac{1}{\delta}\right).$$

We now prove a tighter kl sample compression bound. As our algorithm CoP2L needs two compression sets, we consider a second compression set \mathbf{j} . To use these two compression sets, we need to first redefine the reconstruction function

$$\mathcal{R} : \bigcup_{m \leq n} (\mathcal{X} \times \mathcal{Y})^m \times \bigcup_{k \leq n} (\mathcal{X} \times \mathcal{Y})^k \times \bigcup_{\mathbf{j} \in \mathcal{P}(n)} \mathcal{M}(\mathbf{j}) \rightarrow \Theta.$$

We define a conditional probability distribution $P_{\mathcal{P}(n)}(\mathbf{j} | \mathbf{i})$ that incorporates the knowledge that a vector \mathbf{i} was already drawn from $\mathcal{P}(n)$ and that $\mathbf{i} \cap \mathbf{j} = \emptyset$. Thus, we have $\sum_{\mathbf{i} \in \mathcal{P}(n)} \sum_{\mathbf{j} \in \mathcal{P}(n)} P_{\mathcal{P}(n)}(\mathbf{i}) P_{\mathcal{P}(n)}(\mathbf{j} | \mathbf{i}) \leq 1$. If the choice of \mathbf{j} isn't conditional to the choice of \mathbf{i} , we simply have $P_{\mathcal{P}(n)}(\mathbf{j} | \mathbf{i}) = P_{\mathcal{P}(n)}(\mathbf{j})$.

Theorem C.2. *For any distribution \mathcal{D} over $\mathcal{X} \times \mathcal{Y}$, for any family of set of messages $\{\mathcal{M}(\mathbf{j}) | \mathbf{j} \in \mathcal{P}(n)\}$, for any deterministic reconstruction function \mathcal{R} , for any loss $\ell : \Theta \times \mathcal{X} \times \mathcal{Y} \rightarrow [0, 1]$ and for any $\delta \in (0, 1]$, with probability at least $1 - \delta$ over the draw of $S \sim \mathcal{D}^n$, we have*

$$\forall \mathbf{i} \in \mathcal{P}(n), \mathbf{j} \in \mathcal{P}(n), \mu \in \mathcal{M}(\mathbf{j}) : \\ \mathcal{L}_{\mathcal{D}}(\mathcal{R}(S^{\mathbf{i}}, S^{\mathbf{j}}, \mu)) \leq \text{kl}^{-1}\left(\widehat{\mathcal{L}}_S^{\mathbf{i}^c \cap \mathbf{j}^c}(\mathcal{R}(S^{\mathbf{i}}, S^{\mathbf{j}}, \mu)), \frac{1}{n - |\mathbf{i}| - |\mathbf{j}|} \ln \frac{1}{P_{\mathcal{P}(n)}(\mathbf{i}) P_{\mathcal{P}(n)}(\mathbf{j} | \mathbf{i}) P_{\mathcal{M}(\mathbf{j})}(\mu) \delta}\right)$$

Proof. Let us prove the complement of the expression in Theorem C.2. Denote the upper bound

$$U_{\mathbf{i}, \mathbf{j}, \mu}(\delta) = \text{kl}^{-1}\left(\widehat{\mathcal{L}}_S^{\mathbf{i}^c \cap \mathbf{j}^c}(\mathcal{R}(S^{\mathbf{i}}, S^{\mathbf{j}}, \mu)), \frac{1}{n - |\mathbf{i}| - |\mathbf{j}|} \ln \frac{1}{P_{\mathcal{P}(n)}(\mathbf{i}) P_{\mathcal{P}(n)}(\mathbf{j} | \mathbf{i}) P_{\mathcal{M}(\mathbf{j})}(\mu) \delta}\right).$$

We have

$$\begin{aligned} & \mathbb{P}_{S \sim \mathcal{D}^n} (\exists \mathbf{i}, \mathbf{j} \in \mathcal{P}(n), \mu \in \mathcal{M}(\mathbf{j}) : \mathcal{L}_{\mathcal{D}}(\mathcal{R}(S^{\mathbf{i}}, S^{\mathbf{j}}, \mu)) > U_{\mathbf{i}, \mathbf{j}, \mu}(\delta)) \\ & \leq \sum_{\mathbf{i} \in \mathcal{P}(n)} \sum_{\mathbf{j} \in \mathcal{P}(n)} \mathbb{P}_{S \sim \mathcal{D}^n} (\exists \mu \in \mathcal{M}(\mathbf{j}) : \mathcal{L}_{\mathcal{D}}(\mathcal{R}(S^{\mathbf{i}}, S^{\mathbf{j}}, \mu)) > U_{\mathbf{i}, \mathbf{j}, \mu}(\delta)) \end{aligned} \quad (7)$$

$$\leq \sum_{\mathbf{i} \in \mathcal{P}(n)} \sum_{\mathbf{j} \in \mathcal{P}(n)} \sum_{\mu \in \mathcal{M}(\mathbf{j})} \mathbb{P}_{S \sim \mathcal{D}^n} (\mathcal{L}_{\mathcal{D}}(\mathcal{R}(S^{\mathbf{i}}, S^{\mathbf{j}}, \mu)) > U_{\mathbf{i}, \mathbf{j}, \mu}(\delta)) \quad (8)$$

$$\leq \sum_{\mathbf{i} \in \mathcal{P}(n)} \sum_{\mathbf{j} \in \mathcal{P}(n)} \sum_{\mu \in \mathcal{M}(\mathbf{j})} \mathbb{E}_{S^{\mathbf{i}} \sim \mathcal{D}^{|\mathbf{i}|}} \mathbb{E}_{S^{\mathbf{j}} \sim \mathcal{D}^{|\mathbf{j}|}} \mathbb{P}_{S^{\mathbf{i}^c \cap \mathbf{j}^c} \sim \mathcal{D}^{n - |\mathbf{i}| - |\mathbf{j}|}} (\mathcal{L}_{\mathcal{D}}(\mathcal{R}(S^{\mathbf{i}}, S^{\mathbf{j}}, \mu)) > U_{\mathbf{i}, \mathbf{j}, \mu}(\delta)) \quad (9)$$

$$\leq \sum_{\mathbf{i} \in \mathcal{P}(n)} \sum_{\mathbf{j} \in \mathcal{P}(n)} \sum_{\mu \in \mathcal{M}(\mathbf{j})} \mathbb{E}_{S^{\mathbf{i}} \sim \mathcal{D}^{|\mathbf{i}|}} \mathbb{E}_{S^{\mathbf{j}} \sim \mathcal{D}^{|\mathbf{j}|}} P_{\mathcal{P}(n)}(\mathbf{i}) P_{\mathcal{P}(n)}(\mathbf{j} | \mathbf{i}) P_{\mathcal{M}(\mathbf{j})}(\mu) \delta \quad (10)$$

$$\begin{aligned} & \leq \sum_{\mathbf{i} \in \mathcal{P}(n)} \sum_{\mathbf{j} \in \mathcal{P}(n)} \sum_{\mu \in \mathcal{M}(\mathbf{j})} P_{\mathcal{P}(n)}(\mathbf{i}) P_{\mathcal{P}(n)}(\mathbf{j} | \mathbf{i}) P_{\mathcal{M}(\mathbf{j})}(\mu) \delta \\ & \leq \delta. \end{aligned}$$

Equations (7) and (8) use the union bound, Equation (9) uses the *i.i.d.* assumption, and Equation (10) uses the Chernoff Test-set bound of Theorem C.1 with $p = \mathcal{L}_{\mathcal{D}}(\mathcal{R}(S^{\mathbf{i}}, S^{\mathbf{j}}, \mu)) = \mathbb{E}_{(\mathbf{x}, \mathbf{y}) \sim \mathcal{D}} \ell(\mathcal{R}(S^{\mathbf{i}}, S^{\mathbf{j}}, \mu), \mathbf{x}, \mathbf{y})$ and $X_i = \ell(\mathcal{R}(S^{\mathbf{i}}, S^{\mathbf{j}}, \mu), \mathbf{x}_i, \mathbf{y}_i) \forall i \in \mathbf{i}^c$. Finally, the last inequality is obtained from the definition of $P_{\mathcal{P}(n)}$ and $P_{\mathcal{M}(\mathbf{j})}$. \square

D PROOF OF THEOREM 3.1

Theorem 3.1. For any set of distributions $\{\mathcal{D}_t\}_{t=1}^T$ over $\mathcal{X} \times \mathcal{Y}$ sampled from \mathfrak{D} , and for any $\delta \in (0, 1]$, with probability at least $1 - \delta$ over the draw of $S_{t'} \sim \mathcal{D}_{t'}$, $t' = 1, \dots, T$, we have

$$\forall t \in \{1, \dots, T\}, \mathbf{i}, \mathbf{j} \in \mathcal{P}(n_t), \mu = (\mu_1, \mu_2) \in \mathcal{M}_{1:T}(\mathbf{j}) : \mathcal{L}_{\mathcal{D}_t}(\theta_{\mathbf{i}, \mathbf{j}, \mu}^{(t)}) \leq \text{kl}^{-1} \left(\widehat{\mathcal{L}}_{S_t}^{\mathbf{i}^c \cap \mathbf{j}^c}(\theta_{\mathbf{i}, \mathbf{j}, \mu}^{(t)}), \frac{\epsilon(\mathbf{i}, \mathbf{j}, \mu)}{n_t - |\mathbf{i}| - |\mathbf{j}|} \right),$$

with $\theta_{\mathbf{i}, \mathbf{j}, \mu}^{(t)} = \mathcal{R}_{1:T}(S_t^{\mathbf{i}}, S_t^{\mathbf{j}}, \mu \mid S_1, \dots, S_{t-1}, S_{t+1}, \dots, S_T)$ the reconstructed parameters given by Algorithm 5 and

$$\epsilon(\mathbf{i}, \mathbf{j}, \mu) = \ln \left[\frac{T}{\delta} \binom{n_t}{|\mathbf{i}|} \binom{n_t - |\mathbf{i}|}{|\mathbf{j}|} \frac{(T-1)^{|\mathbf{j}|}}{\zeta(|\mathbf{i}|)\zeta(|\mathbf{j}|)} \prod_{i=1}^T \frac{1}{\zeta(\mu_i^*)} \right].$$

Proof. Let us choose $t \in [1, T]$. Let us sample $S_1, \dots, S_{t-1}, S_{t+1}, \dots, S_T$.

Let

$$U_{\mathbf{i}, \mathbf{j}, \mu}(\delta) = \text{kl}^{-1} \left(\widehat{\mathcal{L}}_S^{\mathbf{i}^c \cap \mathbf{j}^c}(\theta_{\mathbf{i}, \mathbf{j}, \mu}^{(t)}), \frac{1}{n_t - |\mathbf{i}| - |\mathbf{j}|} \ln \frac{1}{P_{\mathcal{P}(n_t)}(\mathbf{i}) P_{\mathcal{P}(n_t)}(\mathbf{j} \mid \mathbf{i}) P_{\mathcal{M}(\mathbf{j})}(\mu) \delta} \right).$$

Then, we have

$$\mathbb{P}_{S^t} \left(\forall \mathbf{i} \in \mathcal{P}(n_t), \mathbf{j} \in \mathcal{P}(n_t), \mu \in \mathcal{M}(\mathbf{j}) : \mathcal{L}_{\mathcal{D}}(\theta_{\mathbf{i}, \mathbf{j}, \mu}^{(t)}) \leq U_{\mathbf{i}, \mathbf{j}, \mu}(\delta) \right).$$

As all the datasets (except S^t) are sampled beforehand, we can define $\mathcal{R}_{1:T}(\cdot) = \mathcal{R}(\cdot; S^1, \dots, S_{t-1}, S_{t+1}, \dots, S_T)$ before drawing S^t . Thus, the reconstruction function is only a function of the dataset S^t , which is the setting of the result of Theorem C.2. We can then lower bound this probability by $1 - \delta$.

We finish the proof by applying the bound to all datasets. We have

$$\begin{aligned} & \mathbb{P}_{S_1, \dots, S_T} \left(\forall \mathbf{i}, \mathbf{j}, \mu : \mathcal{L}_{\mathcal{D}}(\theta_{\mathbf{i}, \mathbf{j}, \mu}^{(t)}) \leq U_{\mathbf{i}, \mathbf{j}, \mu}(\delta) \right) \\ &= \mathbb{E}_{S_1, \dots, S_T} \mathbb{I} \left(\forall \mathbf{i}, \mathbf{j}, \mu : \mathcal{L}_{\mathcal{D}}(\theta_{\mathbf{i}, \mathbf{j}, \mu}^{(t)}) \leq U_{\mathbf{i}, \mathbf{j}, \mu}(\delta) \right) \\ &= \mathbb{E}_{S_1, \dots, S_{t-1}, S_{t+1}, \dots, S_T} \mathbb{E}_{S_t} \mathbb{I} \left(\forall \mathbf{i}, \mathbf{j}, \mu : \mathcal{L}_{\mathcal{D}}(\theta_{\mathbf{i}, \mathbf{j}, \mu}^{(t)}) \leq U_{\mathbf{i}, \mathbf{j}, \mu}(\delta) \right) \\ &= \mathbb{E}_{S_1, \dots, S_{t-1}, S_{t+1}, \dots, S_T} \mathbb{P}_{S_t} \left(\forall \mathbf{i}, \mathbf{j}, \mu : \mathcal{L}_{\mathcal{D}}(\theta_{\mathbf{i}, \mathbf{j}, \mu}^{(t)}) \leq U_{\mathbf{i}, \mathbf{j}, \mu}(\delta) \right) \\ &\geq \mathbb{E}_{S_1, \dots, S_{t-1}, S_{t+1}, \dots, S_T} 1 - \delta \\ &\geq 1 - \delta. \end{aligned}$$

We use a union bound argument to add the $\forall t \in [1, T]$, leading to the term $\frac{\delta}{T}$.

As this theorem holds specifically for CoP2L, we specify the distributions $P_{\mathcal{P}(n_t)}$ and $P_{\mathcal{M}(\mathbf{j})}$. Following the work of Marchand et al. [2003], which used sample compression bounds with three compression sets, with $\zeta(k) = \frac{6}{\pi}(k+1)^{-1}$, we choose

$$P_{\mathcal{P}(n_t)}(\mathbf{i}) = \binom{n_t}{|\mathbf{i}|}^{-1} \zeta(|\mathbf{i}|) \quad \text{and} \quad P_{\mathcal{P}(n_t)}(\mathbf{j} \mid \mathbf{i}) = \binom{n_t - |\mathbf{i}|}{|\mathbf{j}|}^{-1} \zeta(|\mathbf{j}|).$$

Finally, we split the message μ into two messages μ_1 and μ_2 . The first message is defined using the alphabet $\Sigma_1 = \{2, \dots, T\}$. This message indicates the task number where a datapoint is sampled out of the buffer. Thus, the size of Σ_1 is $T - 1$ and the probability of a symbol is $\frac{1}{T-1}$. For any vector \mathbf{j} , we have a sequence of length $|\mathbf{j}|$, and thus the probability of choosing each sequence is $(\frac{1}{T-1})^{|\mathbf{j}|}$.

The second message μ_2 is defined using the alphabet $\Sigma_2 = \{1, \dots, n_t + |\mathcal{B}|\}$. We choose to use $\zeta(k) = \frac{6}{\pi^2}(k+1)^{-2}$ as the probability distribution over each character. We know that for any $N \geq 0$, $\sum_{k=1}^N \zeta(k) \leq 1$. Thus, we have the probability of a sequence $\mu_2 = \mu_2^1 \dots \mu_2^T$ is $\prod_{i=1}^T \zeta(\mu_2^i)$.

We define $\mathcal{M}(\mathbf{j}, T)$ the set of messages such that the sequence of symbols from Σ_1 is of length $|\mathbf{j}|$ and the sequence of symbols from Σ_2 is of length T (Equation 6). \square

E EXPERIMENTS

We denote the licensing information of the principal assets used in this project. Notably, we use Avalanche [Carta et al., 2023] (MIT License), PyTorch [Ansel et al., 2024] (BSD 3-Clause License) and NumPy [Harris et al., 2020] (NumPy license). For the datasets, we use the MNIST dataset [LeCun et al., 1998] (MIT License), the CIFAR10 and CIFAR100 datasets [Krizhevsky, 2012] and subsets of the ImageNet dataset [Deng et al., 2009]. There is no license information for CIFAR10 and CIFAR100, but it is freely available at <https://www.cs.toronto.edu/~kriz/cifar.html> and the authors only ask for their technical report to be cited [Krizhevsky, 2012]. The ImageNet dataset [Deng et al., 2009] and its subsets (TinyImageNet [mnmoustafa and Ali, 2017], ImageNette [Howard, 2019b] and ImageWoof [Howard, 2019a]) are restricted to non-commercial uses and educational purposes².

E.1 DATASET SUMMARY

Datasets used for class incremental learning experiments:

- CIFAR10, 5 tasks of 2 classes each (total of 10 classes)
- CIFAR100 (10 tasks), 10 tasks of 10 classes each (total of 100 classes)
- CIFAR100 (20 tasks), 20 tasks of 5 classes each (total of 100 classes)
- TinyImageNet (40 tasks), 40 tasks of 5 classes each (total of 200 classes)
- ImageNette (5 tasks), 5 tasks of 2 classes each (total of 10 classes)
- ImageWoof (5 tasks), 5 tasks of 2 classes each (total of 10 classes)

E.2 TRAINING, ARCHITECTURE DETAILS AND HYPERPARAMETER SETTINGS FOR THE EXPERIMENTS

Most of our experiments are conducted using the **Avalanche** continual learning framework [Carta et al., 2023], which provides a unified interface for datasets, benchmarks, and baseline implementations. We use the `SimpleMLP` architecture and customized `SimpleCNN` architectures from the Avalanche toolkit for the MNIST, FMNIST, and EMNIST experiments. For CIFAR10, CIFAR100 and TinyImageNet, we use a vision transformer (ViT) [Dosovitskiy et al., 2021], a ResNet50 and a ResNet18 [He et al., 2016]. The first two models are pretrained with Dino [Caron et al., 2021], frozen and followed by a trainable MLP head. ResNet18 was pretrained on ImageNet [Deng et al., 2009], frozen and followed by a trainable MLP head. In the Task-Incremental setting, we follow the pretrained models with a linear layer and a MLP head for each task. All models are trained with a NVIDIA GeForce RTX 4090 GPU using the SGD optimizer.

For all experiments, please refer to Tables 3 to 7 for the hyperparameter configuration. We denote the number of samples added to the compression set at each iteration with k . We denote the weight value used to handle the class-imbalance problem with ω (Both k and ω apply only for the CoP2L (our) algorithm). We also provide the number of epochs, the training batch size and the learning rate for each experiment. For CoP2L, we have chosen the aforementioned hyperparameters by optimizing the performance on the validation set, and for the baseline methods, we have used the hyperparameter values reported in their official implementations. We use $\gamma = -\ln(0.5)$ as stopping criterion for mP2L, as for the cross-entropy loss, this is equivalent to achieving zero errors on the complement set S^{i^c} .

In experiments using a Dino backbone (both ResNet50 and ViT backbones), we upsampled the images to 64x64, since the backbones were pretrained on 224x224 images. We use feature extractors pre-trained on ImageNet using Dino [Caron et al., 2021], which are available on <https://github.com/facebookresearch/dino>. For experiments with a ResNet18, we use a backbone pretrained on ImageNet. For all experiments with pretrained backbones, we freeze the backbone and follow it by a linear head. In Task-Incremental learning, we follow the backbone with a linear layer and a multi-head classification layer, that is a layer that uses a different linear head for each task. We observed better performance from the pretrained feature extractor when the input image size is closer to the original training image size of Dino.

²The licensing information of ImageNet can be found here : <https://image-net.org/download.php>

Table 3: Hyperparameter setup for MNIST, FMNIST and EMNIST using a MLP architecture.

Method	k	ω	Epochs	Batch size	Learning rate
CoP2L	8	15.0	10	256	0.001
Replay	–	–	20	128	0.01
GDumb	–	–	20	128	0.01

Table 4: Hyperparameter setup for MNIST, FMNIST and EMNIST using a CNN architecture.

Method	k	ω	Epochs	Batch size	Learning rate
CoP2L (MNIST & FMNIST)	48	25.0	25	256	0.0009
CoP2L (EMNIST)	105	20.0	15	130	0.0006
Replay	–	–	20	128	0.01
GDumb	–	–	20	128	0.01

Table 5: Hyperparameter setup for Class-Incremental setup.

Method	k	ω	Epochs	Batch size	Learning rate
CoP2L (ViT)	4	25.0	2	256	0.001
Finetuning (ViT)	–	–	20	128	0.01
DER (ViT)	–	–	20	128	0.01
Replay (ViT)	–	–	20	128	0.01
iCaRL (ViT)	–	–	10	128	0.01
GDumb (ViT)	–	–	20	128	0.01
CCLIS (ViT)	–	–	50	512	1.0
CoP2L (RN50)	16	25.0	2	256	0.001
Finetuning (RN50)	–	–	20	128	0.01
DER (RN50)	–	–	20	128	0.01
Replay (RN50)	–	–	20	128	0.01
iCaRL (RN50)	–	–	30	128	0.01
GDumb (RN50)	–	–	20	128	0.01
CCLIS (RN50)	–	–	50	512	1.0
CSReL (RN50)	–	–	100	256	0.001

Table 6: Hyperparameter setup for Task-Incremental setup.

Method	k	ω	Epochs	Batch size	Learning rate
CoP2L (ViT)	4	1.0	2	256	0.001
Finetuning (ViT)	–	–	10	128	0.01
DER (ViT)	–	–	10	128	0.01
Replay (ViT)	–	–	10	128	0.01
LaMAML (ViT)	–	–	10	10	0.01
LwF (ViT)	–	–	10	200	0.001
CCLIS (ViT)	–	–	50	512	1.0
CoP2L (RN50)	16	1.0	2	256	0.001
Finetuning (RN50)	–	–	10	128	0.01
DER (RN50)	–	–	10	128	0.01
Replay (RN50)	–	–	10	128	0.01
LaMAML (RN50)	–	–	10	10	0.01
LwF (RN50)	–	–	10	200	0.001
CCLIS (RN50)	–	–	50	512	1.0
CSReL (RN50)	–	–	100	256	0.001

Table 7: Hyperparameter setup for Domain-Incremental setup (MLP and CNN).

Method	k	ω	Epochs	Batch size	Learning rate
CoP2L	16	15.0	1	256	0.001
Replay	–	–	20	128	0.01
LFL	–	–	3	128	0.01
EWC	–	–	10	256	0.001
SI	–	–	10	256	0.001

E.3 ALL RESULTS WITH STANDARD DEVIATION AND TRAINING TIME

In this section, we provide the average accuracy values obtained on CIFAR10, CIFAR100, TinyImageNet, ImageNette and ImageWoof datasets with the standard deviation estimates. Note that we use different random number generator seeds to account for variability in random number generations (e.g., model parameter initializations) – but train / test splits are kept fixed with respect to seeds across different experiments.

We present new CI results on MNIST, FMNIST and EMNIST, with additional Domain-Incremental (DI) experiments on PermutedMNIST and RotatedMNIST. We evaluate against Replay, Less Forgetful Learning (LFL) [Jung et al., 2018], Elastic Weight Consolidation (EWC) [Kirkpatrick et al., 2017] and Synaptic Intelligence (SI) [Zenke et al., 2017].

Note that, for CIFAR10, CIFAR100, TinyImageNet, ImageWoof, ImageNette, PermutedMNIST and RotatedMNIST experiments we also report the total time it takes to complete each experiment (for all tasks).

E.3.1 Class-Incremental Learning problems

Table 8: Class-incremental learning on CIFAR10 with 5 tasks.

Methods	Average Accuracy (%)	Average Forgetting (%)	Total time (s)
CoP2L (ViT)	94.45 ± 0.14	2.10 ± 0.28	118.07 ± 2.59
Finetuning (ViT)	27.55 ± 1.04	89.74 ± 1.26	880.59 ± 8.33
Replay (ViT)	94.00 ± 0.19	6.11 ± 0.25	486.25 ± 43.07
DER (ViT)	95.03 ± 0.06	3.79 ± 0.15	436.07 ± 1.21
iCaRL (ViT)	88.60 ± 10.04	3.13 ± 4.20	884.59 ± 1.39
GDumb (ViT)	94.16 ± 0.24	3.16 ± 0.39	47.72 ± 0.12
CCLIS (ViT)	93.15 ± 0.34	4.44 ± 0.67	2527.15 ± 44.56
CoP2L (ResNet50)	80.98 ± 0.17	5.84 ± 0.37	527.95 ± 8.43
Finetuning (ResNet50)	19.63 ± 0.02	97.22 ± 0.15	819.80 ± 2.81
Replay (ResNet50)	81.38 ± 0.39	17.72 ± 0.51	287.38 ± 25.06
DER (ResNet50)	82.35 ± 0.22	15.31 ± 0.33	285.65 ± 0.69
iCaRL (ResNet50)	74.49 ± 0.22	1.79 ± 0.43	579.17 ± 2.39
GDumb (ResNet50)	80.84 ± 0.14	9.35 ± 0.30	31.98 ± 0.12
CCLIS (ResNet50)	76.89 ± 0.30	12.32 ± 0.33	2654.32 ± 52.34
CSReL (ResNet50)	34.50 ± 0.29	26.44 ± 0.11	17284.41 ± 157.43

Table 9: Class-incremental learning on CIFAR100 with 10 tasks.

Methods	Average Accuracy (%)	Average Forgetting (%)	Total time (s)
CoP2L (ViT)	73.49 ± 0.27	17.06 ± 0.29	522.18 ± 3.90
Finetuning (ViT)	12.87 ± 0.15	93.27 ± 0.20	901.37 ± 1.73
Replay (ViT)	68.71 ± 0.25	30.02 ± 0.31	453.04 ± 11.93
DER (ViT)	72.29 ± 0.53	25.11 ± 0.53	489.57 ± 7.50
iCaRL (ViT)	65.54 ± 2.23	13.64 ± 0.64	2491.81 ± 2889.82
GDumb (ViT)	72.51 ± 0.26	11.53 ± 0.65	95.43 ± 0.34
CCLIS (ViT)	67.95 ± 0.65	23.68 ± 0.19	3023.03 ± 87.54
CoP2L (ResNet50)	49.53 ± 0.24	22.31 ± 0.20	1724.15 ± 23.50
Finetuning (ResNet50)	9.36 ± 0.05	89.93 ± 0.02	823.61 ± 2.81
Replay (ResNet50)	49.41 ± 0.38	42.12 ± 0.54	295.80 ± 15.88
DER (ResNet50)	49.37 ± 0.16	44.01 ± 0.18	307.86 ± 13.37
iCaRL (ResNet50)	46.06 ± 0.40	8.50 ± 0.28	676.76 ± 56.25
GDumb (ResNet50)	43.37 ± 0.24	20.23 ± 0.42	63.58 ± 0.36
CCLIS (ResNet50)	44.22 ± 0.28	23.23 ± 0.10	3122.45 ± 78.87
CSReL (ResNet50)	38.75 ± 0.25	42.12 ± 0.48	9154.71 ± 278.30

Table 10: Class-incremental learning on CIFAR100 with 20 tasks.

Methods	Average Accuracy (%)	Average Forgetting (%)	Total time (s)
CoP2L (ViT)	70.56 ± 0.99	21.15 ± 2.10	820.66 ± 176.27
Finetuning (ViT)	8.49 ± 0.59	94.64 ± 0.54	902.33 ± 8.58
Replay (ViT)	69.21 ± 0.26	29.52 ± 0.25	457.46 ± 2.07
DER (ViT)	77.03 ± 0.34	19.27 ± 0.48	1096.62 ± 19.46
iCaRL (ViT)	62.36 ± 1.46	15.88 ± 0.84	1359.13 ± 4.58
GDumb (ViT)	72.35 ± 0.30	11.77 ± 0.40	190.80 ± 0.42
CCLIS (ViT)	66.81 ± 0.34	24.42 ± 0.29	3947.38 ± 89.23
CoP2L (ResNet50)	46.74 ± 1.63	22.54 ± 0.92	1771.12 ± 757.50
Finetuning (ResNet50)	4.88 ± 0.03	92.81 ± 0.31	1247.98 ± 506.91
Replay (ResNet50)	49.44 ± 0.30	44.96 ± 0.36	293.25 ± 1.77
DER (ResNet50)	57.53 ± 0.05	33.37 ± 0.05	510.52 ± 99.48
iCaRL (ResNet50)	46.47 ± 0.33	6.74 ± 0.31	858.11 ± 120.41
GDumb (ResNet50)	43.60 ± 0.38	19.93 ± 0.56	126.74 ± 0.46
CCLIS (ResNet50)	39.10 ± 0.04	25.78 ± 0.03	4021.21 ± 59.34
CSReL (ResNet50)	32.57 ± 0.02	40.23 ± 0.27	13404.29 ± 320.31

Table 11: Class-incremental learning on TinyImageNet with 40 tasks.

Methods	Average Accuracy (%)	Average Forgetting (%)	Total time (s)
CoP2L (ViT)	51.59 ± 0.24	36.32 ± 0.29	1451.93 ± 4.71
Finetuning (ViT)	2.83 ± 0.17	95.36 ± 0.31	2304.54 ± 37.18
Replay (ViT)	47.49 ± 0.47	48.39 ± 0.49	1128.97 ± 16.95
DER (ViT)	53.92 ± 0.36	41.77 ± 0.45	1280.76 ± 131.53
iCaRL (ViT)	21.06 ± 1.11	34.49 ± 9.37	3919.23 ± 2170.08
GDumb (ViT)	53.93 ± 0.34	15.11 ± 0.19	471.23 ± 17.85
CCLIS (ViT)	48.55 ± 0.46	32.26 ± 0.43	8000.69 ± 355.45
CoP2L (ResNet50)	33.30 ± 0.32	35.93 ± 0.27	3671.69 ± 29.19
Finetuning (ResNet50)	1.80 ± 0.36	78.66 ± 1.04	2167.76 ± 161.91
Replay (ResNet50)	28.38 ± 0.42	63.36 ± 0.44	882.12 ± 180.18
DER (ResNet50)	28.77 ± 0.34	64.17 ± 0.34	818.11 ± 10.28
iCaRL (ResNet50)	33.89 ± 0.47	10.42 ± 0.44	1905.26 ± 295.18
GDumb (ResNet50)	24.29 ± 0.58	21.29 ± 0.56	332.22 ± 0.98
CCLIS (ResNet50)	18.32 ± 0.11	40.40 ± 0.02	8349.31 ± 378.39
CSReL (ResNet50)	12.84 ± 0.22	73.69 ± 0.40	39644.46 ± 237.23

Table 12: Class-incremental learning on MNIST with 5 tasks.

Methods	Average Accuracy (%)	Average Forgetting (%)
CoP2L (MLP)	95.12 \pm 0.18	3.35 \pm 0.24
Replay (MLP)	94.48 \pm 0.28	6.08 \pm 0.32
GDumb (MLP)	91.70 \pm 0.31	3.84 \pm 0.29
CoP2L (CNN)	96.61 \pm 0.07	2.16 \pm 0.28
Replay (CNN)	96.93 \pm 0.29	3.31 \pm 0.38
GDumb (CNN)	94.41 \pm 0.13	2.97 \pm 0.46

Table 13: Class-incremental learning on Fashion-MNIST with 5 tasks.

Methods	Average Accuracy (%)	Average Forgetting (%)
CoP2L (MLP)	84.23 \pm 0.27	12.10 \pm 0.66
Replay (MLP)	83.99 \pm 0.52	15.92 \pm 0.42
GDumb (MLP)	81.76 \pm 0.36	10.44 \pm 0.50
CoP2L (CNN)	87.35 \pm 0.15	11.12 \pm 0.36
Replay (CNN)	87.59 \pm 0.11	13.32 \pm 0.29
GDumb (CNN)	84.98 \pm 0.21	8.78 \pm 0.41

Table 14: Class-incremental learning on EMNIST with 13 tasks.

Methods	Average Accuracy (%)	Average Forgetting (%)
CoP2L (MLP)	78.03 \pm 0.17	16.67 \pm 0.31
Replay (MLP)	77.22 \pm 0.44	22.08 \pm 0.50
GDumb (MLP)	62.64 \pm 0.20	15.96 \pm 0.58
CoP2L (CNN)	87.90 \pm 0.41	8.38 \pm 0.54
Replay (CNN)	87.70 \pm 0.50	12.29 \pm 0.49
GDumb (CNN)	85.05 \pm 0.27	7.50 \pm 0.61

E.3.2 Task-Incremental Learning problems

Table 15: Task-incremental learning on CIFAR10 with 5 tasks.

Methods	Average Accuracy (%)	Average Forgetting (%)	Total time (s)
CoP2L (ViT)	99.04 ± 0.05	-0.00 ± 0.10	64.51 ± 0.68
Finetuning (ViT)	99.15 ± 0.06	0.23 ± 0.04	466.97 ± 11.76
Replay (ViT)	99.29 ± 0.04	-0.01 ± 0.03	217.83 ± 0.76
DER (ViT)	99.15 ± 0.08	0.21 ± 0.05	133.94 ± 1.02
LaMAML (ViT)	99.25 ± 0.06	0.05 ± 0.07	344.65 ± 1.46
LwF (ViT)	97.89 ± 0.41	1.69 ± 0.48	165.41 ± 0.75
CCLIS (ViT)	98.81 ± 0.89	0.48 ± 0.12	2534.15 ± 53.56
CoP2L (ResNet50)	96.22 ± 0.18	0.56 ± 0.28	172.51 ± 4.42
Finetuning (ResNet50)	96.60 ± 0.08	1.00 ± 0.11	460.78 ± 3.38
Replay (ResNet50)	96.88 ± 0.06	0.42 ± 0.13	144.57 ± 0.51
DER (ResNet50)	96.57 ± 0.10	1.09 ± 0.14	90.56 ± 0.36
LaMAML (ResNet50)	96.65 ± 0.21	0.73 ± 0.21	310.51 ± 1.64
LwF (ResNet50)	95.80 ± 0.15	0.33 ± 0.20	97.09 ± 0.21
CCLIS (ResNet50)	95.45 ± 0.02	0.79 ± 0.13	2637.16 ± 61.23
CSReL (ResNet50)	65.46 ± 0.56	13.66 ± 0.19	12354.00 ± 160.45

Table 16: Task-incremental learning on CIFAR100 with 10 tasks.

Methods	Average Accuracy (%)	Average Forgetting (%)	Total time (s)
CoP2L (ViT)	95.03 ± 0.08	0.90 ± 0.11	290.95 ± 30.98
Finetuning (ViT)	95.17 ± 0.11	1.84 ± 0.13	478.64 ± 6.32
Replay (ViT)	96.43 ± 0.14	0.34 ± 0.17	235.81 ± 1.10
DER (ViT)	96.22 ± 0.12	0.71 ± 0.13	137.12 ± 1.96
LaMAML (ViT)	95.58 ± 0.16	0.58 ± 0.12	397.78 ± 3.40
LwF (ViT)	95.09 ± 0.10	0.98 ± 0.10	173.57 ± 0.63
CCLIS (ViT)	90.99 ± 0.45	4.49 ± 0.69	2532.34 ± 49.57
CoP2L (ResNet50)	86.78 ± 0.16	2.01 ± 0.17	435.10 ± 7.74
Finetuning (ResNet50)	88.23 ± 0.09	1.78 ± 0.08	430.99 ± 2.11
Replay (ResNet50)	87.61 ± 0.05	0.86 ± 0.16	157.05 ± 0.14
DER (ResNet50)	88.29 ± 0.20	1.72 ± 0.28	91.77 ± 1.07
LaMAML (ResNet50)	83.57 ± 0.43	6.18 ± 0.53	357.24 ± 4.58
LwF (ResNet50)	79.39 ± 0.13	0.47 ± 0.11	101.27 ± 0.48
CCLIS (ResNet50)	78.55 ± 0.09	6.76 ± 0.21	2659.12 ± 43.02
CSReL (ResNet50)	69.14 ± 0.14	15.17 ± 0.41	5670.32 ± 256.32

Table 17: Task-incremental learning with CIFAR100 with 20 tasks.

Methods	Average Accuracy (%)	Average Forgetting (%)	Total time (s)
CoP2L (ViT)	97.18 \pm 0.13	0.56 \pm 0.18	226.65 \pm 21.43
Finetuning (ViT)	97.57 \pm 0.23	0.86 \pm 0.22	473.71 \pm 6.70
Replay (ViT)	98.09 \pm 0.09	0.25 \pm 0.12	250.78 \pm 1.45
DER (ViT)	98.08 \pm 0.10	0.31 \pm 0.17	137.98 \pm 0.24
LaMAML (ViT)	97.84 \pm 0.10	0.26 \pm 0.14	448.43 \pm 2.81
LwF (ViT)	95.74 \pm 0.19	2.15 \pm 0.21	180.36 \pm 0.98
CCLIS (ViT)	94.86 \pm 0.54	2.88 \pm 0.45	3951.13 \pm 68.94
CoP2L (ResNet50)	90.89 \pm 0.22	2.27 \pm 0.28	278.67 \pm 6.20
Finetuning (ResNet50)	93.25 \pm 0.04	1.27 \pm 0.06	436.93 \pm 2.10
Replay (ResNet50)	92.89 \pm 0.18	0.47 \pm 0.24	167.65 \pm 1.26
DER (ResNet50)	93.43 \pm 0.02	1.11 \pm 0.05	94.25 \pm 0.30
LaMAML (ResNet50)	89.89 \pm 0.75	4.12 \pm 0.78	407.84 \pm 7.38
LwF (ResNet50)	87.73 \pm 0.18	0.33 \pm 0.23	105.46 \pm 0.49
CCLIS (ResNet50)	83.51 \pm 0.14	6.60 \pm 0.11	4079.41 \pm 61.34
CSReL (ResNet50)	63.52 \pm 0.32	14.49 \pm 0.22	8364.45 \pm 289.56

Table 18: Task-incremental learning on TinyImageNet with 40 tasks.

Methods	Average Accuracy (%)	Average Forgetting (%)	Total time (s)
CoP2L (ViT)	93.81 \pm 0.26	1.50 \pm 0.28	1039.14 \pm 146.21
Finetuning (ViT)	93.62 \pm 0.20	2.61 \pm 0.21	983.62 \pm 9.49
Replay (ViT)	95.66 \pm 0.08	0.50 \pm 0.09	632.18 \pm 2.97
DER (ViT)	95.08 \pm 0.07	1.13 \pm 0.15	316.37 \pm 0.81
LaMAML (ViT)	94.82 \pm 0.23	0.79 \pm 0.19	1527.24 \pm 891.43
LwF (ViT)	85.18 \pm 0.76	9.72 \pm 0.71	430.63 \pm 2.14
CCLIS (ViT)	86.82 \pm 0.23	6.14 \pm 0.56	8012.79 \pm 321.46
CoP2L (ResNet50)	88.57 \pm 0.17	2.46 \pm 0.19	890.94 \pm 3.44
Finetuning (ResNet50)	90.62 \pm 0.35	1.38 \pm 0.40	905.9 \pm 10.10
Replay (ResNet50)	90.03 \pm 0.26	1.26 \pm 0.27	514.42 \pm 102.82
DER (ResNet50)	90.66 \pm 0.06	1.12 \pm 0.15	237.61 \pm 1.12
LaMAML (ResNet50)	87.20 \pm 0.34	4.53 \pm 0.28	1268.50 \pm 551.93
LwF (ResNet50)	85.03 \pm 0.17	0.89 \pm 0.21	284.79 \pm 5.67
CCLIS (ResNet50)	75.65 \pm 0.05	14.12 \pm 0.31	8379.89 \pm 381.29
CSReL (ResNet50)	50.22 \pm 0.21	22.34 \pm 0.51	21455.97 \pm 231.76

Table 19: Task-incremental learning on ImageNette with 5 tasks.

Methods	Average Accuracy (%)	Average Forgetting (%)	Total time (s)
CoP2L (ViT)	98.22 \pm 0.19	-0.43 \pm 0.12	118.71 \pm 24.35
Finetuning (ViT)	98.24 \pm 0.22	0.53 \pm 0.17	221.15 \pm 2.16
Replay (ViT)	98.61 \pm 0.03	-0.02 \pm 0.10	356.58 \pm 2.89
LaMAML (ViT)	98.42 \pm 0.02	0.03 \pm 0.00	309.91 \pm 5.42
LwF (ViT)	96.51 \pm 0.67	1.97 \pm 0.79	164.80 \pm 1.90

Table 20: Task-incremental learning on ImageWoof with 5 tasks.

Methods	Average Accuracy (%)	Average Forgetting (%)	Total time (s)
CoP2L (ViT)	93.34 \pm 0.30	-0.65 \pm 0.40	246.77 \pm 13.43
Finetuning (ViT)	93.20 \pm 0.49	2.00 \pm 0.84	201.91 \pm 1.89
Replay (ViT)	94.29 \pm 0.30	0.16 \pm 0.26	316.87 \pm 0.93
LaMAML (ViT)	94.00 \pm 0.21	0.12 \pm 0.38	276.19 \pm 3.45
LwF (ViT)	89.75 \pm 1.88	5.76 \pm 2.61	175.82 \pm 39.30

E.3.3 Domain-Incremental Learning problems

Table 21: Domain-incremental learning on Permuted-MNIST with 10 tasks.

Methods	Average Accuracy (%)	Average Forgetting (%)	Total time (s)
CoP2L (MLP)	91.61 ± 0.39	6.69 ± 0.40	1381.06 ± 1232.99
Replay (MLP)	91.28 ± 0.18	6.75 ± 0.21	1128.99 ± 49.82
LFL (MLP)	82.76 ± 1.23	10.15 ± 1.36	92.86 ± 0.24
EWC (MLP)	82.53 ± 0.82	6.50 ± 0.88	340.16 ± 3.81
SI (MLP)	85.85 ± 0.61	11.69 ± 0.67	319.95 ± 1.38

Table 22: Domain-incremental learning on Rotated-MNIST on 10 tasks.

Methods	Average Accuracy (%)	Average Forgetting (%)	Total time (s)
CoP2L (MLP)	89.40 ± 1.00	8.71 ± 1.04	4970.86 ± 1452.34
Replay (MLP)	88.75 ± 0.67	9.53 ± 0.72	3894.62 ± 75.11
LFL (MLP)	53.09 ± 7.06	44.18 ± 7.93	387.61 ± 160.54
EWC (MLP)	55.59 ± 5.57	36.58 ± 6.27	1133.19 ± 18.10
SI (MLP)	59.90 ± 6.48	41.38 ± 7.18	1043.86 ± 7.28

E.4 BOUND PLOTS

E.4.1 Bound plots for different buffer sizes

This section presents the computed bound values over task risks on MNIST, Fashion-MNIST and EMNIST datasets (letters) in Class-Incremental settings. Figure 4 shows results for different replay buffer sizes (1000, 2000, 3000, 4000, 5000) obtained using the MLP architecture. Figure 5 shows the results obtained with the CNN architecture. We report the estimated deviation of the bound values over different seeds using the shaded regions which show the ± 1 standard deviation, and also the whiskers (plotted using the seaborn toolkit's boxplot function) which show the spread of the values excluding the outliers. This plotting style for showing the deviation across seeds applies to all bound plots presented in this paper.

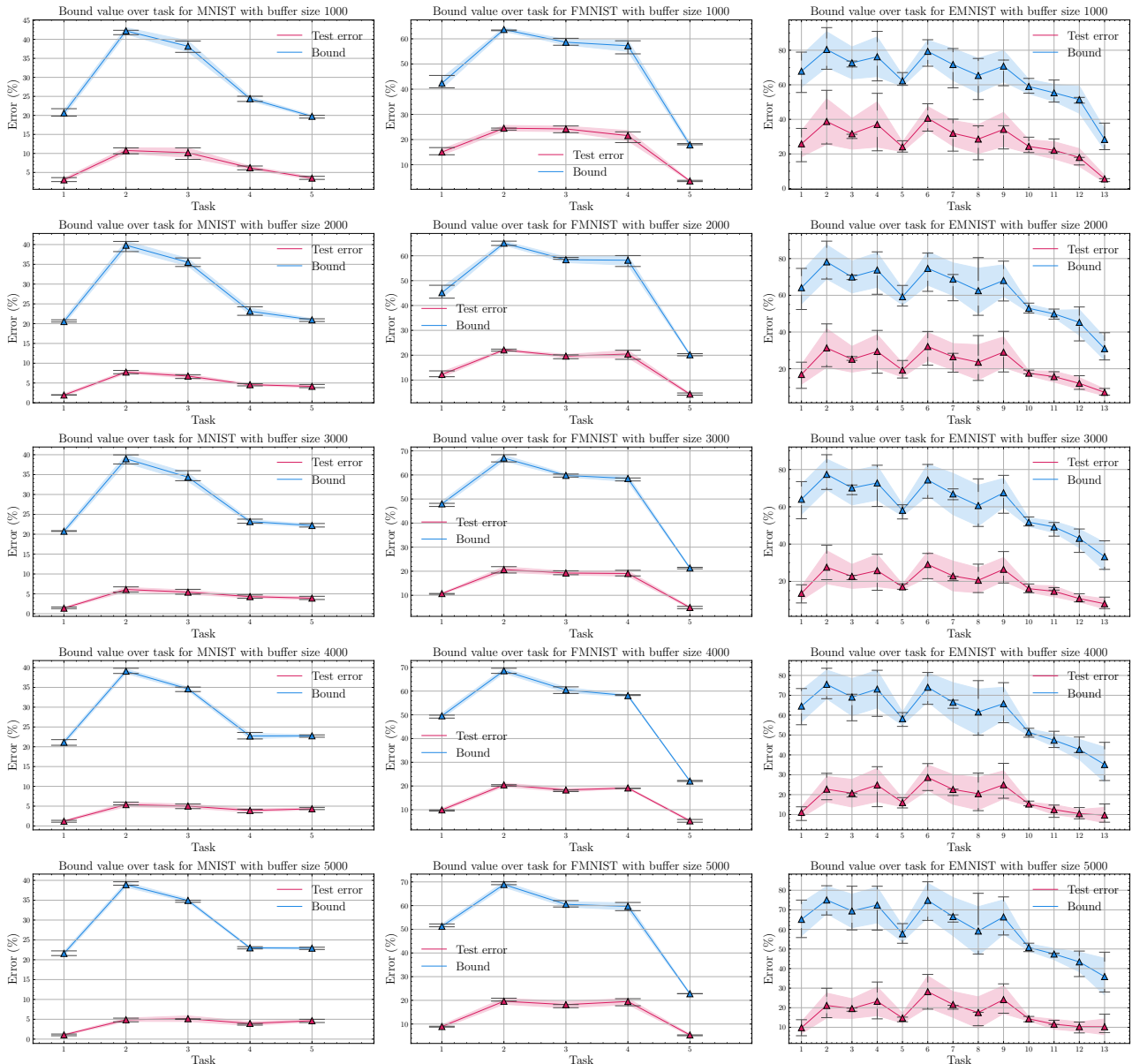


Figure 4: CoP2L Bounds with respect to tasks on the MNIST, Fashion-MNIST and EMNIST datasets using an MLP architecture

We observe from Figures 4 and 5 that the MLP architecture and the CNN architecture give non-trivial bounds that follow the trends exhibited by the test error curve.

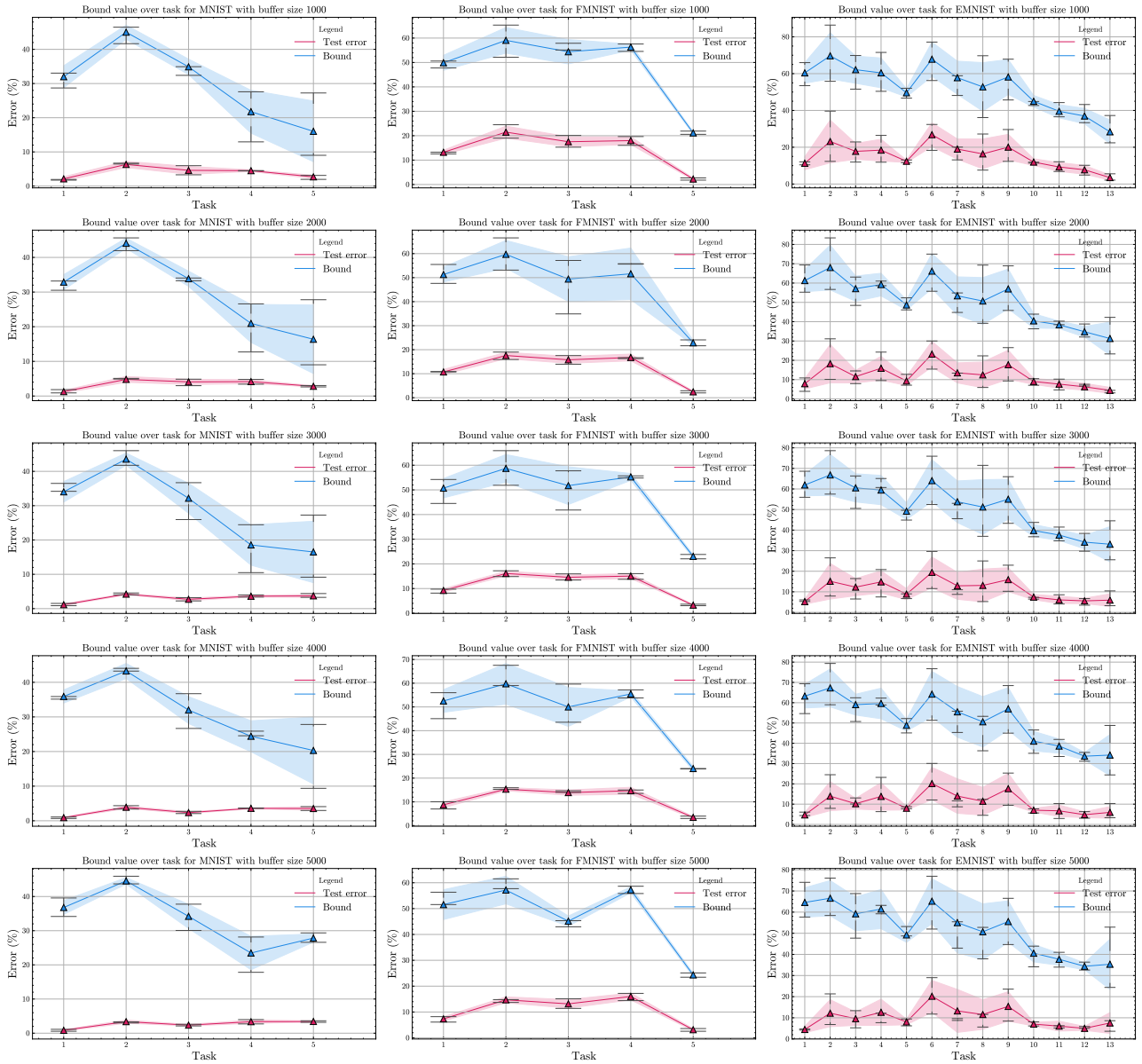


Figure 5: CoP2L Bounds with respect to tasks on the MNIST, Fashion-MNIST and EMNIST datasets using a CNN architecture

E.4.2 Bound plots for CIFAR10, CIFAR100, TinyImageNet and ImageNet (subsets) datasets

In this section, we present the plots for the bound values obtained for the additional datasets, namely CIFAR10, CIFAR100, and ImageNet subsets. The ImageNet subsets include the Tinyimagenet [mnmoustafa and Ali, 2017], ImageWoof [Howard, 2019a], and ImageNette [Howard, 2019b] datasets. We provide the results on ImageWoof and ImageNette to showcase that the estimated bounds get tighter when more data is available per each task.

We note that as the pretrained models used as backbones for our experiments were pretrained on the ImageNet, we provide the bounds on the ImageNet subsets simply to give insight to the reader. Indeed, the dependency of the backbones to the dataset over which we certify breaks the *i.i.d.* assumption of the bound.

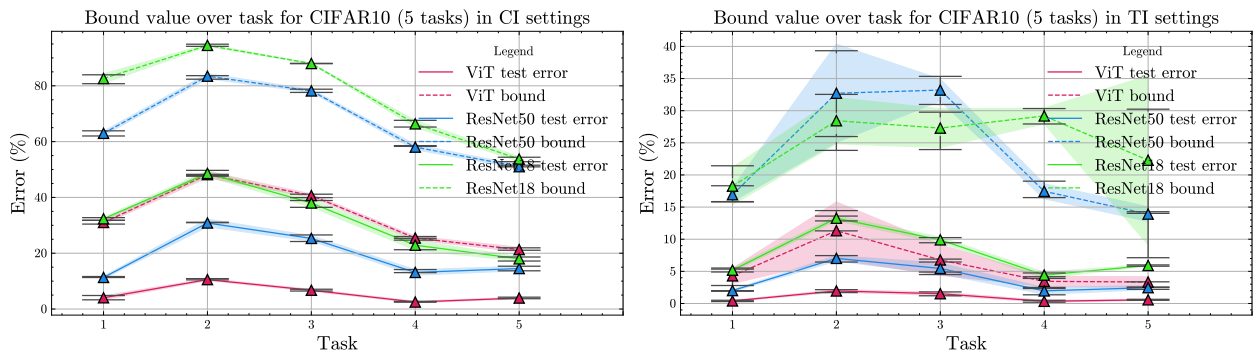


Figure 6: CoP2L bounds with respect to tasks on the CIFAR10 (5 tasks) dataset in Class-Incremental (left) and Task-Incremental (right) settings

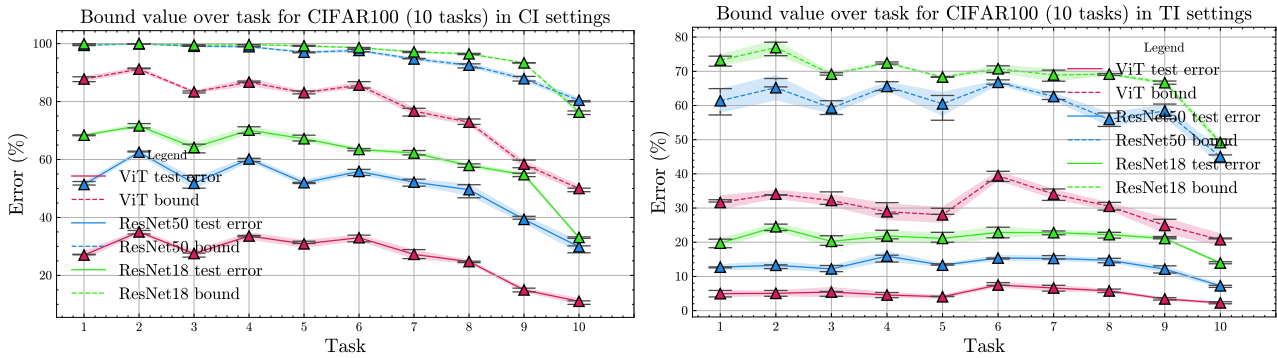


Figure 7: CoP2L bounds with respect to tasks on the CIFAR100 (10 tasks) dataset in Class-Incremental (left) and Task-Incremental (right) settings

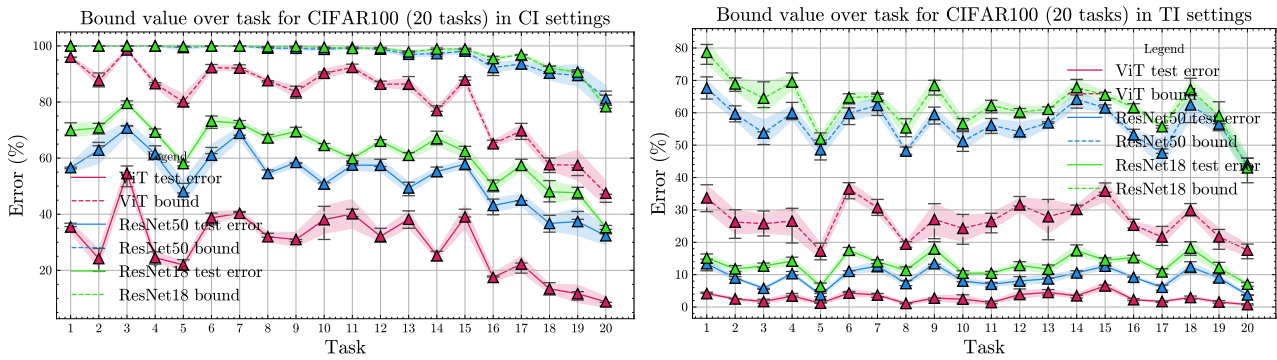


Figure 8: CoP2L bounds with respect to tasks on the CIFAR100 (20 tasks) dataset in Class-Incremental (left) and Task-Incremental (right) settings

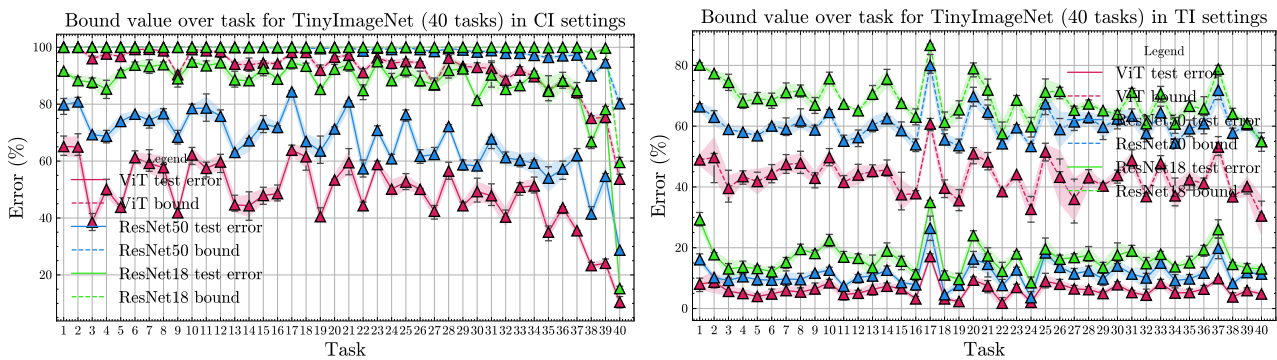


Figure 9: CoP2L bounds with respect to tasks on the TinyImageNet (40 tasks) dataset in Class-Incremental (left) and Task-Incremental (right) settings

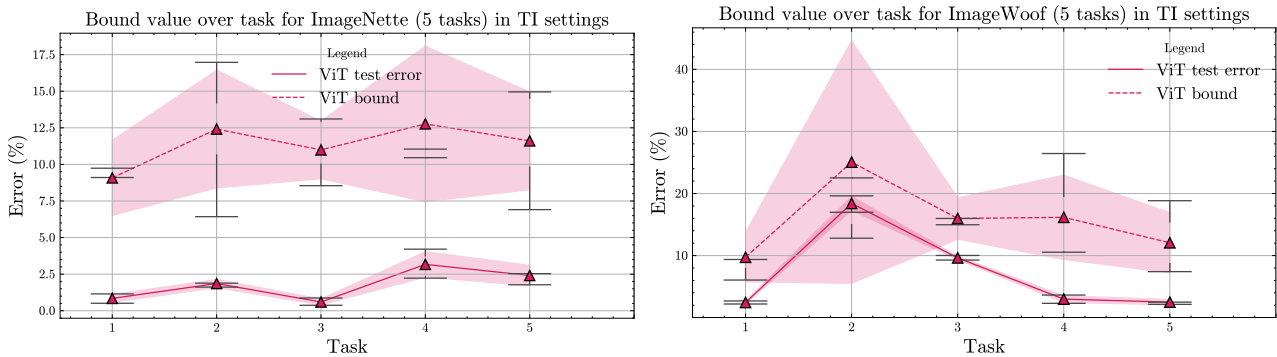


Figure 10: CoP2L bounds with respect to tasks on the ImageNette (5 tasks) dataset (left) and ImageWoof dataset (right) in Task-Incremental setting

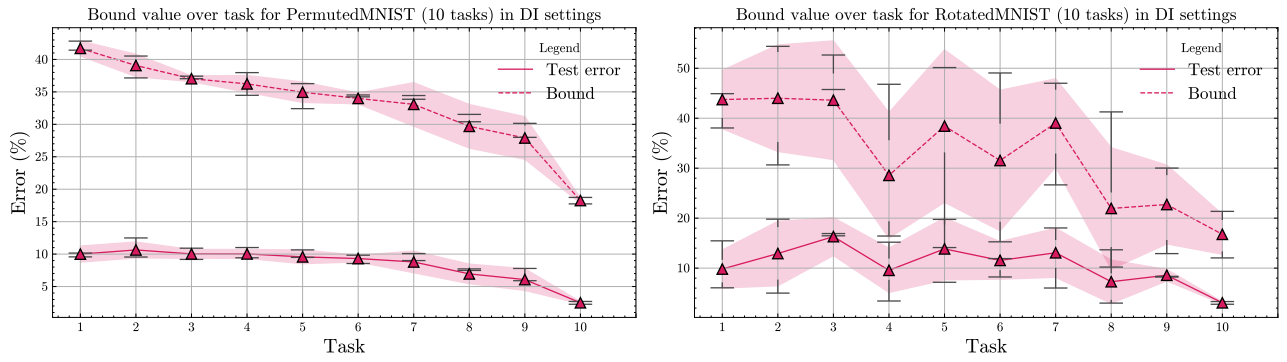


Figure 11: CoP2L bounds with respect to tasks on the PermutatedMNIST (10 tasks) dataset (left) and on the RotatedMNIST dataset in Domain-Incremental setting

F ANALYSIS OF COP2L

In this section we provide multiple analyses and ablation studies of CoP2L.

F.1 ABLATION ON COP2L LOSS TERMS.

We have conducted an ablation study to understand the effect of additional weighting that counteracts class imbalance that arises in the continual learning setup when new tasks are introduced (Standard replay counteracts this by extending the batch size to have equal class representation). In the modified P2L (Algorithm 2), we incorporate an additional weighting term over classes to adapt P2L for class-balanced continual learning. In order to assess whether this idea is indeed helpful, we have run an experiment on the MNIST dataset with and without the additional weighting idea. In Figure 12, we show the results of this experiment. For both accuracy (left panel) and forgetting (right panel), we observe that the inclusion of the additional loss weighting term significantly improves the results.

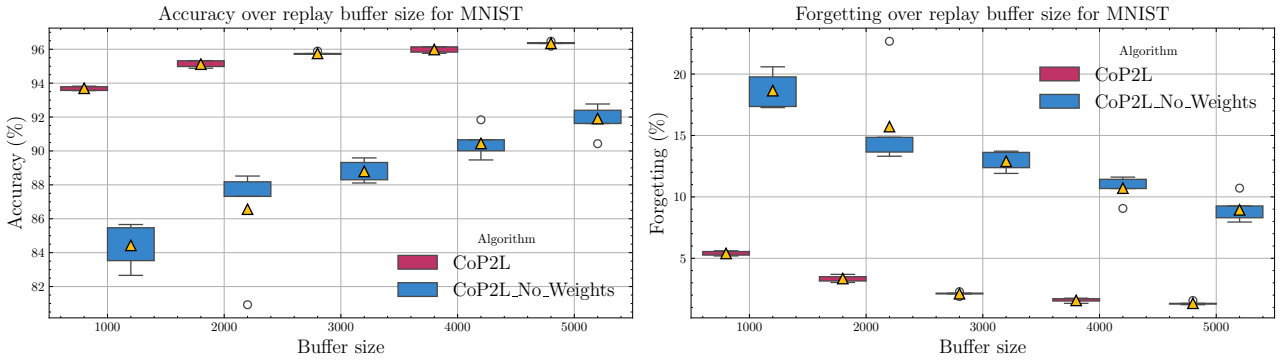


Figure 12: Ablation study on MNIST and Fashion-MNIST on the additional weighting to ensure class balance we propose in Algorithm 2 on the CoP2L loss function. Accuracy (**left**) and forgetting (**right**) over replay buffer size for the MNIST dataset

F.2 SENSITIVITY ANALYSIS WITH RESPECT TO THE TASK ORDERING.

In order to also assess the sensitivity of CoP2L with respect to ordering of the tasks, on MNIST and Fashion-MNIST experiments we have conducted an experiment where we randomly shuffle the task order. For both datasets, we have tested our algorithm with 5 different random task ordering. For each task, we report the cumulative accuracy such that, Average Cumulative $Acc_{.T} = \frac{1}{O \cdot T} \sum_{o=1}^O \sum_{t=1}^T Accuracy_{T,t}^o$, where $Accuracy_{T,t}^o$ denotes the accuracy obtained at task t after finishing training until task T , and the o index denotes the task order. We have used $O = 5$ different task orderings. We present the results of this experiment in Figure 13. On both MNIST and Fashion-MNIST datasets CoP2L is able to outperform with more tasks. We also observe that the variability of the results decrease more significantly for CoP2L compared to replay.

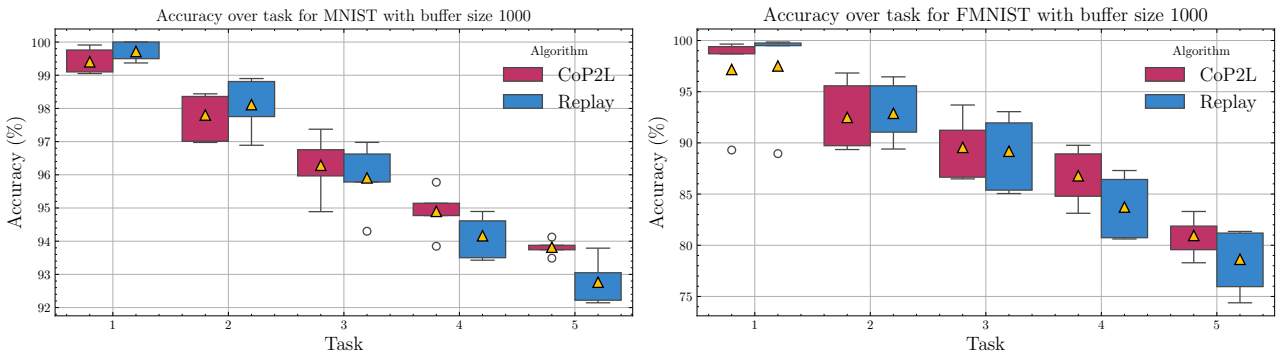


Figure 13: Studying the variation of cumulative accuracy with respect to task ordering for CoP2L and Replay on MNIST dataset (**left**) and Fashion-MNIST dataset (**right**). We use 5 different task order, and show the variability with respect to each task.

E.3 ANALYSIS WITH RESPECT TO BUFFER SIZE

In Fig. 14, we compare the accuracy and forgetting obtained with replay buffer sizes of 1000–5000 samples for CoP2L and replay. This corresponds to roughly 8–40% of the per-task dataset size for MNIST and Fashion-MNIST, and 10–52% for EMNIST. We report the final average accuracy (after $T=5$ tasks for MNIST and Fashion-MNIST, and $T=13$ for EMNIST) across seeds as well as per-task test accuracy.

For MNIST, CoP2L clearly outperforms replay on average. For Fashion-MNIST and EMNIST, CoP2L shows a clear advantage for small buffers and remains comparable or slightly better for larger buffers. Across all datasets, CoP2L substantially reduces forgetting.

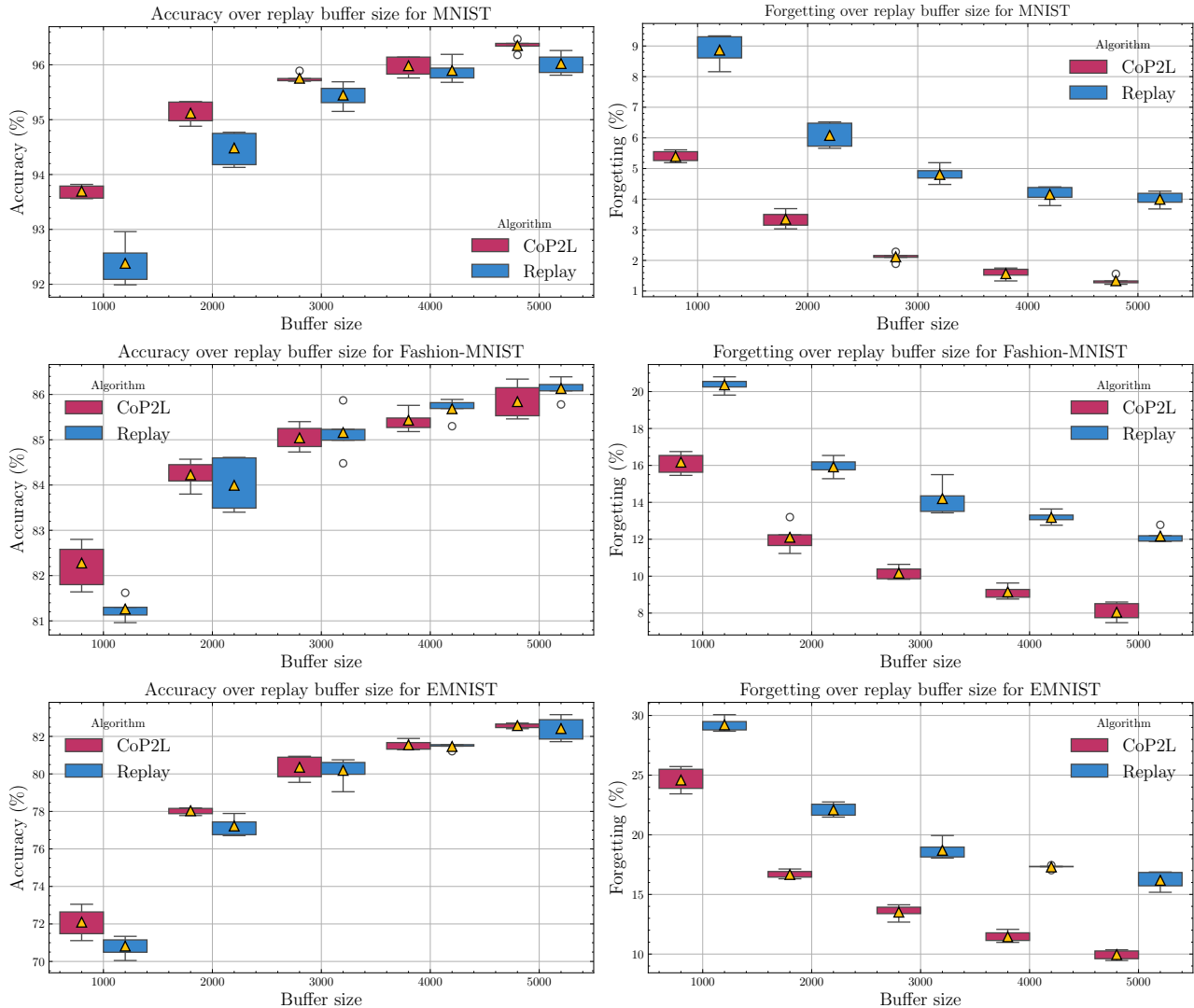


Figure 14: Accuracy (left) and forgetting (right) vs. buffer size for MNIST (top), Fashion-MNIST (middle), and EMNIST (bottom). Orange triangles indicate mean performance.

E.4 ANALYSIS OF MEMORY COST

We have conducted a memory comparison on Split-CIFAR10 (5 tasks) in Class Incremental Learning (CIL) and Task Incremental Learning (TIL) settings, as shown in Table 23.

We report Maximum allocated memory (actual usage), maximum reserved memory (allocated memory PyTorch’s caching allocator), and also the average cumulative memory over all tasks.

We would like to note that, in the current implementation, we execute the sample compression in one go, by processing all data items that correspond to the current task in parallel. It is totally possible to implement this with minibatching without

loss of performance. The table reports, in parentheses, the approximate memory that would be used by CoP2L using the same minibatch size as the reported Replay.

Table 23: Memory usage comparison for CoP2L and Replay in CIL and TIL settings.

Method	Max Mem allocated (MB)	Max Mem reserved (MB)	Cumulate Mem usage (TB)
CIL			
CoP2L	15535.57 ± 87.53 (342.85 ± 6.34)	22310.0 ± 104.67 (492.36 ± 7.98)	1261.38 ± 31.72
Replay	458.76 ± 9.84	648.0 ± 12.35	3383.43 ± 74.51
TIL			
CoP2L	15535.66 ± 98.34 (342.86 ± 6.78)	22310.0 ± 102.65 (492.36 ± 7.81)	197.18 ± 6.42
Replay	458.85 ± 9.91	648.0 ± 12.41	1783.11 ± 52.63

F.5 ABLATION ON THE USE OF EARLY STOPPING

In this section, we study the use of early stopping in our CoP2L algorithm. We present the result in Table 24. The early stopping improves the accuracy, the forgetting and the bound on each task except for the bound on Task 1 with the ViT. This is to be expected as the early stopping helps to alleviate the overfitting of Pick-To-Learn by selecting the checkpoint that achieves the best bound once the algorithm has effectively converged. In contrast, without early stopping, training proceeds until the training error reaches zero, which can lead to overfitting, bigger compression set and consequently worse generalization metrics. This can also explain the tighter bounds, as it was demonstrated by Bazinet et al. [2025] that, on binary subsets of the MNIST dataset, the sample-compression bound was actually minimized about halfway before Pick-To-Learn converges.

Table 24: Illustration of the behavior of the bound on CIFAR10 after 5 tasks, with and without early stopping using the bound.

	Backbone	Accuracy (↑)	Forgetting (↓)	Bound on Task 1 (↓)	Bound on Task 2 (↓)	Bound on Task 3(↓)	Bound on Task 4(↓)	Bound on Task 5(↓)
With early stopping	RN18	68.12 ± 0.42	17.62 ± 0.31	82.34 ± 0.55	94.62 ± 0.47	88.17 ± 0.36	66.15 ± 0.28	53.52 ± 0.44
	RN50	80.98 ± 0.25	5.84 ± 0.18	62.97 ± 0.63	83.46 ± 0.39	78.17 ± 0.41	58.03 ± 0.22	51.02 ± 0.35
	ViT	94.45 ± 0.12	2.10 ± 0.09	31.02 ± 0.48	48.17 ± 0.33	40.66 ± 0.27	25.45 ± 0.19	21.30 ± 0.26
Without early stopping	RN18	65.30 ± 0.51	22.71 ± 0.37	90.02 ± 0.46	96.67 ± 0.40	91.20 ± 0.35	71.06 ± 0.29	59.15 ± 0.43
	RN50	77.36 ± 0.34	12.11 ± 0.26	78.05 ± 0.52	91.65 ± 0.38	83.52 ± 0.31	60.04 ± 0.24	53.28 ± 0.36
	ViT	94.34 ± 0.11	2.63 ± 0.07	29.46 ± 0.45	49.46 ± 0.30	42.16 ± 0.28	25.99 ± 0.21	23.72 ± 0.25

F.6 CLASS-WISE ACCURACY

We report the accuracies obtained over earlier tasks with CoP2L and with replay. We observe that CoP2L is able to obtain a more balanced performance over earlier tasks compared to standard replay, as can be seen from the last rows of Table 25, and Table 26.

Table 25: The accuracies obtained on earlier tasks with CoP2L on CIFAR10.

	Class 1	Class 2	Class 3	Class 4	Class 5	Class 6	Class 7	Class 8	Class 9	Class 10
Task 1	98.10 ± 0.22	97.30 ± 0.31								
Task 2	98.60 ± 0.18	96.80 ± 0.27	83.70 ± 0.45	85.50 ± 0.36						
Task 3	95.70 ± 0.29	96.70 ± 0.21	79.40 ± 0.52	77.40 ± 0.47	82.90 ± 0.33	71.10 ± 0.58				
Task 4	93.50 ± 0.34	97.00 ± 0.19	72.60 ± 0.49	68.70 ± 0.55	84.10 ± 0.28	71.20 ± 0.46	84.40 ± 0.31	80.10 ± 0.37		
Task 5	85.30 ± 0.41	91.50 ± 0.26	71.40 ± 0.53	66.50 ± 0.60	80.20 ± 0.35	69.70 ± 0.48	90.30 ± 0.24	83.60 ± 0.39	89.50 ± 0.30	83.10 ± 0.42

Table 26: The accuracies obtained on earlier tasks with standard replay algorithm on CIFAR10.

	Class 1	Class 2	Class 3	Class 4	Class 5	Class 6	Class 7	Class 8	Class 9	Class 10
Task 1	98.10 ± 0.24	98.40 ± 0.19								
Task 2	93.10 ± 0.38	97.20 ± 0.27	94.70 ± 0.33	92.40 ± 0.41						
Task 3	93.80 ± 0.36	96.80 ± 0.22	74.90 ± 0.55	53.80 ± 0.61	94.70 ± 0.29	90.50 ± 0.34				
Task 4	91.70 ± 0.40	96.50 ± 0.25	70.90 ± 0.57	57.20 ± 0.63	69.80 ± 0.48	76.20 ± 0.45	96.30 ± 0.21	95.60 ± 0.26		
Task 5	77.30 ± 0.52	77.90 ± 0.49	73.00 ± 0.54	59.90 ± 0.60	75.10 ± 0.47	80.90 ± 0.39	92.00 ± 0.28	87.70 ± 0.36	98.20 ± 0.18	96.10 ± 0.23

E.7 PLASTICITY FORGETTING TRADEOFF

Denoting $A(t, \theta_t)$ the accuracy obtained on a task t of a model f_{θ_t} after finishing training on task t , the plasticity is given by

$$\bar{P}(\theta_T) = \frac{1}{T} \sum_{t=1}^T A(t, \theta_t),$$

We observe that CoP2L is able to retain a low level of forgetting while having a relatively good level of plasticity. As shown in Table 27, CoP2L consistently attains substantially lower forgetting than Finetuning, Replay, and Dark Experience Replay, and also outperforms GDumb on this metric. Although iCaRL achieves slightly lower forgetting, this comes at the cost of reduced plasticity. Overall, this trade-off highlights the favorable balance achieved by CoP2L. We observe the same behavior across both RN50 and ViT backbones.

Table 27: Plasticity vs Forgetting Tradeoff on CIFAR10 dataset

Backbone	Method	Plasticity (\uparrow)	Forgetting (\downarrow)
RN50	CoP2L	85.57 ± 0.34	5.55 ± 0.28
RN50	Finetuning	97.21 ± 0.22	97.22 ± 0.41
RN50	Replay	95.50 ± 0.37	17.09 ± 0.33
RN50	iCaRL	75.79 ± 0.45	1.54 ± 0.19
RN50	Gdumb	87.86 ± 0.31	8.95 ± 0.36
RN50	DER	94.78 ± 0.27	15.60 ± 0.42
ViT	CoP2L	96.33 ± 0.18	3.36 ± 0.21
ViT	Finetuning	99.36 ± 0.09	89.74 ± 0.38
ViT	Replay	98.82 ± 0.14	6.01 ± 0.26
ViT	iCaRL	94.48 ± 0.23	1.55 ± 0.17
ViT	Gdumb	96.86 ± 0.20	3.39 ± 0.24
ViT	DER	98.09 ± 0.16	3.86 ± 0.29